Acta Neuropathologica (2024) 148:76
https://doi.org/10.1007/s00401-024-02832-9

ORIGINAL PAPER

Raphe and ventrolateral medulla proteomics in sudden unexplained death in childhood with febrile seizure history

Dominique F. Leitner[1,2,3] · Christopher William[2,4] · Arline Faustin[2,3,4] · Evgeny Kanshin[5] · Matija Snuderl[4] · Declan McGuone[6] · Thomas Wisniewski[2,3,4,8] · Beatrix Ueberheide[2,5,7] · Laura Gould[2,9] · Orrin Devinsky[1,2]

Received: 27 August 2024 / Revised: 28 October 2024 / Accepted: 11 November 2024

Abstract

Sudden unexplained death in childhood (SUDC) is death of a child ≥ 12 months old that is unexplained after autopsy and detailed analyses. Among SUDC cases, ~ 30% have febrile seizure (FS) history, versus 2–5% in the general population. SUDC cases share features with sudden unexpected death in epilepsy (SUDEP) and sudden infant death syndrome (SIDS), in which brainstem autonomic dysfunction is implicated. To understand whether brainstem protein changes are associated with FS history in SUDC, we performed label-free quantitative mass spectrometry on microdissected midbrain dorsal raphe, medullary raphe, and the ventrolateral medulla (n = 8 SUDC-noFS, n = 11 SUDC-FS). Differential expression analysis between SUDC-FS and SUDC-noFS at $p < 0.05$ identified 178 altered proteins in dorsal raphe, 344 in medullary raphe, and 100 in the ventrolateral medulla. These proteins were most significantly associated with increased eukaryotic translation initiation ($p = 3.09 \times 10^{-7}$, z = 1.00), eukaryotic translation elongation ($p = 6.31 \times 10^{-49}$, z = 6.01), and coagulation system ($p = 1.32 \times 10^{-5}$, z = 1.00). The medullary raphe had the strongest enrichment for altered signaling pathways, including with comparisons to three other brain regions previously analyzed (frontal cortex, hippocampal dentate gyrus, cornu ammonus). Immunofluorescent tissue analysis of serotonin receptors identified 2.1-fold increased 5HT2A in the medullary raphe of SUDC-FS ($p = 0.025$). Weighted gene correlation network analysis (WGCNA) of case history indicated that longer FS history duration significantly correlated with protein levels in the medullary raphe and ventrolateral medulla; the most significant gene ontology biological processes were decreased cellular respiration ($p = 9.8 \times 10^{-5}$, corr = − 0.80) in medullary raphe and decreased synaptic vesicle cycle ($p = 1.60 \times 10^{-7}$, corr = − 0.90) in the ventrolateral medulla. Overall, FS in SUDC was associated with more protein differences in the medullary raphe and was related with increased translation-related signaling pathways. Future studies should assess whether these changes result from FS or may in some way predispose to FS or SUDC.

Keywords SUDC · Febrile seizures · Proteomics · Laser capture microdissection

✉ Orrin Devinsky
Orrin.Devinsky@nyulangone.org

1 Comprehensive Epilepsy Center, NYU Grossman School of Medicine, New York, NY, USA

2 Department of Neurology, NYU Grossman School of Medicine, New York, NY, USA

3 Center for Cognitive Neurology, NYU Grossman School of Medicine, New York, NY, USA

4 Department of Pathology, NYU Grossman School of Medicine, New York, NY, USA

5 Proteomics Laboratory, Division of Advanced Research Technologies, NYU Grossman School of Medicine, New York, NY, USA

6 Department of Pathology, Yale School of Medicine, New Haven, CT, USA

7 Department of Biochemistry and Molecular Pharmacology, NYU Grossman School of Medicine, New York, NY, USA

8 Department of Psychiatry, NYU Grossman School of Medicine, New York, NY, USA

9 Sudden Unexplained Death in Childhood Foundation, New Jersey, USA

Published online: 28 November 2024

Introduction

Sudden unexplained death in childhood (SUDC) is death of a child ≥ 12 months old for whom the cause of death (COD) is unexplained after autopsy and detailed analyses [9]. In typical cases, death occurs in sleep and the child is prone; there is a male predominance [24, 25, 32, 48]. Among SUDC cases, febrile seizure (FS) history occurs in 28.8% of the SUDC Foundation cohort versus 2–5% of the general population [16]. Unwitnessed and undiagnosed FS may occur in SUDC cases with terminal seizures during sleep [17]. These characteristics parallel those in sudden unexpected death in epilepsy (SUDEP) and sudden infant death syndrome (SIDS) [1, 11, 25, 31–33], and share neuropathological and other features [23, 32, 39, 40, 48, 51, 69]. Previous neuropathology studies have observed findings in SUDC cases that were similar to temporal lobe epilepsy [23, 32, 34, 48], although some of these findings occur in explained COD cases and thus additional studies are needed to provide consensus on the variation in the normal range of hippocampal anatomy as well as brainstem [42, 47, 63]. Further, our recent proteomic analyses of SUDC cases indicated more protein differences in the frontal cortex than in the hippocampus, a region that does not frequently contain detectable neuropathology [44]. The combination of these characteristics implicate brainstem dysfunction leading to autonomic disorders that may be the final common path for most neurologically mediated sudden deaths. Brainstem nuclei initiate and regulate respiration (e.g., midbrain dorsal raphe modulates arousal response to hypercapnia [27, 30, 56, 67]; medial medullary raphe regulate respiration via chemoreceptors [4, 61]; the ventrolateral medullary pre-Botzinger complex coordinates respiratory rhythm [56, 64]). In SIDS, reduced medullary serotonergic receptor binding activity may impair respiratory function [31, 33]. In SUDEP cases, we found protein changes in these brainstem regions [40]. To understand whether these regions are impacted in SUDC cases with FS (SUDC-FS), we performed localized proteomic analyses to identify altered proteins and the associated signaling pathways. This builds on our findings of protein changes in frontal cortex and hippocampus of SUDC cases [44].

Methods

Human brain tissue Autopsy brain tissue was obtained through the multisite collaboration with the SUDC Registry and Research Collaborative (SUDCRRC), approved by the New York University School of Medicine Institutional Review Board (IRB #14–01061). SUDCRRC evaluates cases ages 1 month to 18 years old who died suddenly and unexpectedly and the COD is unexplained after autopsy and complete forensic assessment [9]; all performed before proteomic analyses. Cases were referred from multiple sites, including NYU, Columbia University, the Mayo Clinic (Minnesota), and ≥ 30 clinical and forensic collaborators at medical examiner and coroner offices. Consent for SUDC cases was provided by the decedent's parent(s)/guardian(s). After brain tissue was obtained, neuropathological examination was performed, and brain tissue was processed into FFPE blocks. Neuropathology findings were described [44, 48] and are summarized in Table 2 and detailed in Supplementary Table 1. SUDC cases with or without FS history were included from those enrolled in the SUDCRRC from 2015 to 2018, and with brainstem regions of interest in formalin less than 3 years. FS history included either simple or complex FS, with simple FS being generalized and lasting less than 15 min while complex FS are seizures lasting more than 15 min and recurring within 24 h [66]. Cases were excluded (n = 3) when ancillary analyses identified potential pathogenic whole exome sequencing (WES) variants that may contribute to COD [20]. Various microbiology testing was performed at autopsy as we note in our previous study of the same cases [44], with 4/17 tested cases with positive post-mortem virology from respiratory and brain samples that were considered not to contribute to COD. Cohort demographics and post mortem data from the cases with (SUDC-FS) and without (SUDC-noFS) FS history are summarized in Table 1, detailed in Table 2 and Supplementary Table 1; these cases were evaluated in our proteomic analyses of other brain regions [44].

Brainstem nuclei identification All brain tissue was evaluated before LCM to confirm brain regions of interest as described [40]. Midbrain at the level of the inferior colliculus was evaluated by immunofluorescence (IF) on a parallel glass slide before LCM to confirm that the tryptophan hydroxylase positive (TPH2(+)) neurons of the dorsal raphe were present, as this region may not be present in bisected tissue or rostral to the inferior colliculus. The medulla at 4 levels within 1 cm above obex were evaluated for the TPH2(+) neurons of the medullary raphe and NK1R(+) cells of the ventrolateral medulla. All tissue processing and sectioning was performed by the NYU Center for Biospecimen Research and Development. For IF, 8 µm sections were deparaffinized and rehydrated through a series of xylenes and ethanol, followed by heat-induced antigen retrieval with 10 mM sodium citrate, 0.05% triton-×100 at pH 6. After blocking in 10% normal donkey serum, sections were incubated overnight at 4 °C with primary antibodies for TPH2 (1:250, Abcam ab121013) for midbrain or TPH2 and NK1R (1:100, Sigma S8305) for medulla. Secondary antibodies

Table 1 Cohort demographics and post mortem data

Group	Cases	Mean age at death (years)	Sex	Mean PMI (hours)	Mean brain weight (grams)
Midbrain dorsal raphe					
SUDC-noFS	7	3.4 ± 3.8	1 F / 6 M	30 ± 25	1228 ± 144
SUDC-FS	9	2.7 ± 0.8	6 F / 3 M	37 ± 32	1266 ± 83
Medullary Raphe					
SUDC-noFS	8	5.0 ± 5.6	2 F / 6 M	31 ± 23	1265 ± 168
SUDC-FS	9	2.8 ± 0.9	6 F / 3 M	42 ± 32	1267 ± 101
Ventrolateral medulla					
SUDC-noFS	8	5.0 ± 5.6	2 F / 6 M	31 ± 23	1265 ± 168
SUDC-FS	11	2.8 ± 0.8	8 F / 3 M	39 ± 29	1269 ± 90

included donkey anti-goat Alexa-Fluor 488 (1:500, Thermofisher) and donkey anti-rabbit Alexa-Fluor 555 (1:500, ThermoFisher), with nuclei counterstaining by Hoescht (Sigma B2261).

LCM After confirming brainstem nuclei localization, tissue was dissected from sections at one level of the brainstem at 8 µm on LCM compatible PET slides (Leica), after being sectioned onto slides by NYU Experimental Pathology. LCM slides were subjected to IF for TPH2 or NK1R/TPH2 (antibodies described above), as described [40]. For the ventrolateral medulla, an overview scan for the entire section before LCM allowed for NK1R(+) and anatomical localization. From each region, 12 mm^2 of the ventrolateral medulla bilaterally, and 4.5 mm^2 for the midbrain dorsal raphe and medullary raphe were microdissected into LC–MS grade water (Thermo Scientific). Protein quantification from equal areas for each case allows for protein quantification with very low protein concentrations (estimated at < 1 ug protein/sample). Microdissected samples were centrifuged for 2 min at 14,000 *g* and stored at − 80˚C. LCM was performed at 5X magnification with a Leica LMD6500 microscope equipped with a UV laser. Schematic of targeted regions was partially generated in Biorender (Fig. 1).

LFQ-MS Proteins were extracted using SPEED-based protocol. FFPE samples were incubated in 10 ul of TFA for 3 min at 73C with subsequent 10x (v:v) dilution in 2 M TRIS containing 10 mM TCEP and 20 mM CAA and additional incubation at 90 C for 1 h. After 6x (v:v) dilution with water containing 0.2 ug of sequencing-grade trypsin (Promega), proteins were digested overnight at 37 C. The resulting peptide samples were acidified with TFA (to final 2%) and loaded on Evosep Pure C18 tips. LC separation was performed online on Evosep One LC utilizing Dr Maisch C18 AQ, 1.9 µm beads (150 µm ID, 15 cm long, cat# EV-1106) analytical column. Peptides were gradient eluted from the column directly to Q-Exactive Orbitrap HF-X mass spectrometer using 88 min extended Evosep method (SPD15) at a flowrate of 220 nl/min. The mass spectrometer was operated in data-independent acquisition mode (DIA), doing MS^2 fragmentation across 22 m/z windows after every MS^1 scan event. High resolution full MS spectra were acquired with a resolution of 120,000, an AGC target of 3e6, with a maximum ion injection time of 60 ms, and scan range of 350–1650 m/z. Following each full MS scan 22 data-independent HCD MS/MS scans were acquired at the resolution of 30,000, AGC target of 3e6, stepped nce of 22.5, 25 and 27.5.

MS data were analyzed using Spectronaut software (https://biognosys.com/shop/spectronaut) and searched in directDIA mode against the *Homo sapiens* reference proteome database (http://www.uniprot.org/) including protein isoforms. Database searches were performed in integrated search engine Pulsar. For searching, the enzyme specificity was set to trypsin with the maximum number of missed cleavages set to 2. Oxidation of methionine was searched as variable modification; carbamidomethylation of cysteines was searched as a fixed modification. The false discovery rate (FDR) for peptide, protein, and site identification were set to 1%. Quantification was performed on MS^2 level using 3 most intense fragment ions per precursor. Raw MS data were deposited on the MassIVE server (https://massive.ucsd.edu/) under accession MSV000095576.

Data were log transformed and normalized using median intensity across all samples. The protein expression matrix (n = 2,923) was filtered to contain only proteins that were quantified in at least half the cases in one group (SUDC-FS or SUDC-noFS) in each brain region (midbrain dorsal raphe: n = 2,813; medullary raphe: n = 2,819; ventrolateral medulla: n = 2,826). For principal component analysis (PCA), missing values were imputed from the normal distribution with a width of 0.3 and downshift of 1.8 (relative to measured protein intensity distribution) in Perseus [71]. Unpaired t-tests were performed in Perseus to detect significant changes in protein expression between SUDC-FS and SUDC-noFS. Significance was $p < 0.05$. Cell type annotations were derived from a reference data

Table 2 Case history [44]

Case ID	Age (yr)	Sex	Other medical history	Febrile seizure history	Apparent terminal activity	Found body position	PMI (hr)	Brain weight (grams)	Significant neuropathology
1	1.45	F	Fever 24 h	Simple	Sleep	Prone	55	1200	Mild hippocampal microscopic abnormalities; early acute hypoxic-ischemic neuronal damage
2	1.79	M	Fever 24 h, Mild motor/speech delay, autism spectrum	Simple	Sleep	Prone	35	1320	Mild hippocampal microscopic abnormalities and mild reactive changes
3	1.83	F	Fever 24–72 h, virus detected	Simple	Sleep	Prone	29	1180	
4	3.48	F		Simple	Sleep	Prone	30	1173	
5	1.48	F	Fever 24–72 h	None	Sleep	Prone	12	1241	
6	3.33	F	Speech delay	Complex	Sleep	Prone	9	1220	
7	2.90	F	Frequent URIs, pneumonia	Simple	Sleep	Prone	61	1170	
8	2.73	M		Simple	Sleep	Prone	112	1310	
9	1.85	M	Fever 24–72 h, virus detected	None	Sleep	Prone	20	1234	Left hippocampal asymmetry and dilated perivascular spaces
10	2.39	M		None	Sleep	Prone	18	1220	Bilateral hippocampal abnormalities, mild
11	2.58	M	Asthma, reactive airway disease, frequent URIs, Mild motor/speech delay, poor visual function	None	Sleep	Prone	15	1210	Hippocampal abnormalities, mild
12	2.88	F	Fever 24–72 h, Mild motor/speech delay	Simple	Sleep	Prone	38	1275	Mild reactive change
13	2.82	F	Fever 24–72 h, virus detected, mild sleep apnea, reactive airway disease	Complex	Rest	Prone	17	1286	
14	3.72	M	Reactive airway disease	Simple	Sleep	Supine	8	1430	
15	15.98	F	Asthma, reactive airway disease, respiratory infections	None	Sleep	Prone	38	1520	Focal cortical dysplasia, type IIA; hippocampal dysgenesis
16	1.18	M		None	Sleep	Side	26	945	
17	3.58	F	Fever 24–72 h, virus detected	Simple	Sleep	Prone	36	1400	Hippocampal abnormalities, mild
18	11.84	M	Asthma, multiple URIs	None	Sleep	Side	83	1390	Diffuse edema
19	2.61	M	Fever 72 h	None	Sleep	Prone	37	1358	Diffuse edema and hippocampal malrotation with variation in the thickness of the dentate gyrus

URI upper respiratory infection, *yr* years, *hr* hours, *PMI* post-mortem interval

set [36] and as described [40, 43, 59], with 1066 possible annotations from gene IDs that were associated with one cell type. Overlap in proteins of interest were evaluated by Venn diagram generated from InteractiVenn [22]. Correlation analyses were performed by Pearson correlation in GraphPad Prism.

Pathway analysis The signaling pathways associated with protein differences were evaluated by Ingenuity Pathway Analysis (IPA; Qiagen). A Core Analysis for each brain region had a threshold for each protein at $p < 0.05$. The top 20 pathways are in a bubble plot produced in GraphPad Prism and Adobe Illustrator, with z-score in blue (decreased)

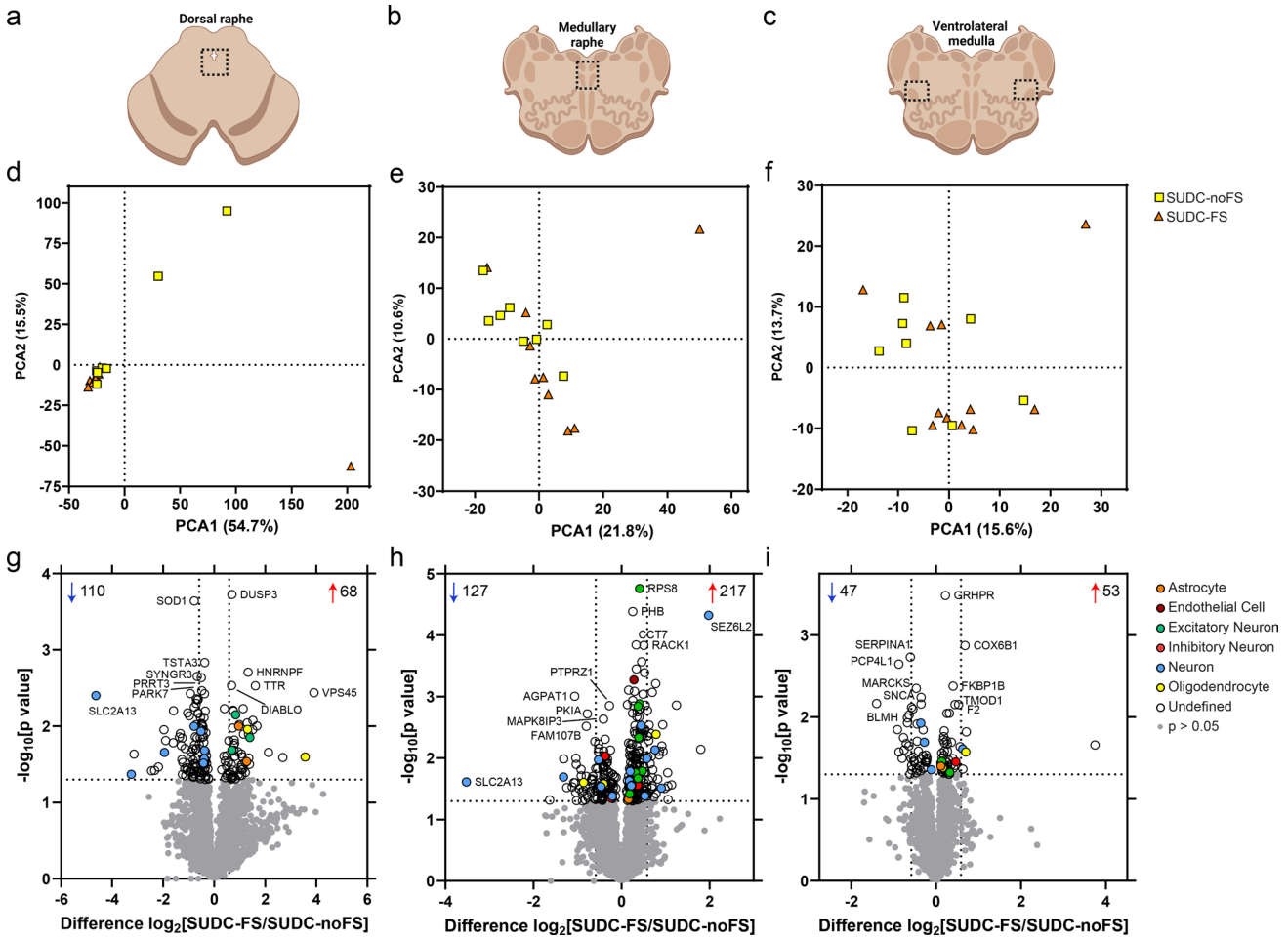

Fig. 1 Dissected brainstem regions and differential expression analyses. **a**–**c**) overview schematic of regions microdissected in the midbrain dorsal raphe, medullary raphe, and ventrolateral medulla. After proteomic analysis, principal component analysis (PCA) shows distribution of SUDC cases with febrile seizure history (SUDC-FS; orange) and SUDC cases without febrile seizure history (SUDC-noFS; yellow) in the midbrain dorsal raphe **d**), medullary raphe **e**), and ventrolateral medulla **f**). There was no segregation of cases by FS history in any of the brain regions analyzed, in PCA1: midbrain dorsal raphe ($p=0.93$, unpaired t-test), medullary raphe ($p=0.12$), ventrolateral medulla ($p=0.24$) or PCA2: midbrain dorsal raphe ($p=0.055$), medullary raphe ($p=0.33$), ventrolateral medulla ($p=0.72$). **g**) Differential expression analysis identified 178 altered proteins (68 increased, 110 decreased) in the midbrain dorsal raphe at $p<0.05$. **h** In the medullary raphe, 344 proteins were altered (217 increased, 127 decreased). **i** In the ventrolateral medulla, 100 proteins were altered (53 increased, 47 decreased). The top 5 significantly increased and decreased proteins are annotated by gene name, as well as protein of interest SLC2A13. Dotted lines correspond to $p<0.05$ and fold change at 1.5. Cell type annotation for each protein is indicated by color. Additional protein information is available in Supplementary Tables 2, 3, 4

and red (increased). White color indicates z-score that was "NA" or z = 0.

Weighted gene correlation network analysis (WGCNA) WGCNA evaluated protein correlations with clinical variables (see Supplementary Table 1) in the R environment with the *WGCNA* package for blockwise Modules with defaults as described [28, 37, 41, 44, 65] except where noted. Soft threshold power beta was $R^2=0.8$. The power for each brain region: midbrain dorsal raphe = 5, medullary raphe = 5, and ventrolateral medulla = 7. Gene ontology (GO) annotations for modules was determined following WGCNA with the *anRichment* package in the R environment with Entrez IDs against the human GOcollection. GO annotations were considered with an FDR < 5% and associated with at least 5 proteins.

Immunofluorescence (IF) IF was performed to evaluate top protein candidates identified by proteomics (SEZ6L2, SLC2A13), as well as other related serotonin receptor proteins (5HT1A, 5HT2A) in all cases evaluated by proteomics. SEZ6L2 and SLC2A13 antibodies were selected with consultation from Protein Atlas (www.proteinatlas.org) that has a growing tissue database characterizing antibodies, with the SEZ6L2 and SLC2A13 antibodies having an "enhanced – orthogonal" rating for IHC as antibody staining is mainly

consistent with RNA expression across 45 tissues. The 5HT1A and 5HT2A antibodies have been used previously in various experimental approaches in our and other studies [2, 38, 45, 53, 60, 76]. 8 µm FFPE sections were deparaffinized and rehydrated in a series of xylenes and ethanol dilutions. After washing, heat-induced antigen retrieval was performed with 10 mM sodium citrate, 0.05% triton-×100 pH 6. Tissue was blocked with 10% normal donkey serum, followed by overnight incubation at 4 °C with primary antibodies SEZ6L2 (1:100, Sigma HPA064471), SLC2A13 (1:100, Sigma HPA061679), TPH2 (1:250, Abcam ab121013), 5HT1A (1:100, Abcam ab227165), and 5HT2A (1:100, Santa Cruz sc-166775). After washes, sections were incubated with corresponding secondary antibodies, donkey anti-goat Alexa-Fluor 488, donkey anti-rabbit Alexa-Fluor 647, donkey anti-mouse Alexa-Fluor 647 (1:500, ThermoFisher). Sections were counterstained with DAPI (Sigma D9542) and coverslipped. Whole slide images were acquired using a Leica Aperio Versa 8 Scanner at 20X magnification with the same settings for each slide, including representative images. There were 1–4 images for midbrain dorsal raphe and 1–2 images for medullary raphe or ventrolateral medulla collected for each case, excluding any tissue artifact. Images were analyzed in Fiji ImageJ with the same binary threshold for all images to determine the number of positive pixels in each ROI corresponding to regions analyzed by proteomics, an average percentage of the total image area. From the same images, colocalization analyses were performed to determine the Mander coefficient for each channel with the Colocalization Threshold plugin in Fiji ImageJ. The same ROIs and thresholds for the single channel analyses were used to calculate the Mander coefficient [13]. The Mander coefficient was averaged across available images for each case, followed by statistical comparison in each channel (i.e. SUDC-FS (red) vs SUDC-noFS (red); SUDC-FS (green) vs SUDC-noFS (green)). Unpaired t-tests were performed for statistical analysis, with $p < 0.05$ considered significant.

Results

Case history

SUDC cases were evaluated with FS history (SUDC-FS; n = 11) and without FS history (SUDC-noFS; n = 8; Tables 1, 2, Supplementary Table 1), with no significant age difference; most SUDC-FS cases were female. Among the SUDC-FS cases, 2 cases had complex FS and the remaining 9 cases had simple FS. FS onset averaged 20 months of age (range 13–30 months), and FS history duration averaged 13 (range 0.5–26.6 months). FS occurred within three months of death in 3 cases. Fever within 24 h of death occurred in 4/11 SUDC-FS and 2/8 SUDC-noFS cases ($p > 0.99$, Fisher's exact test). Fever within 72 h of death occurred in 6/11 SUDC-FS and 3/8 SUDC-noFS cases ($p = 0.65$). Virus was detected in 3/10 SUDC-FS and 1/7 SUDC-noFS cases when tested ($p = 0.60$). Neuropathology was unremarkable in all cases; no brainstem diagnostic macroscopic or microscopic abnormalities were identified.

Proteomics differential expression analysis

The midbrain dorsal raphe, medullary raphe, and ventrolateral medulla were microdissected when available (Fig. 1a–c). PCA did not indicate segregation by FS history in any brain regions (Fig. 1d–f). There were several cases with more variability within a group, with one SUDC-FS case indicating more differences than other cases in both medullary regions. In the midbrain dorsal raphe from SUDC-FS (n = 9) and SUDC-noFS (n = 7), 2813 proteins were detected in ≥ 50% of the groups (Supplementary Table 2). In the medullary raphe from SUDC-FS (n = 9) and SUDC-noFS (n = 8), 2819 proteins were detected in ≥ 50% of the groups (Supplementary Table 3). In the ventrolateral medulla from SUDC-FS (n = 11) and SUDC-noFS (n = 8), there were 2826 proteins detected in ≥ 50% of one of the groups (Supplementary Table 4).

Differential expression analysis between SUDC-FS and SUDC-noFS ($p < 0.05$) identified 178 altered proteins in the midbrain dorsal raphe, 344 proteins in the medullary raphe, and 100 proteins in the ventrolateral medulla (Fig. 1g–i, Supplementary Tables 2, 3, 4). Tables 3, 4, 5 summarize the top 20 significant proteins in each brain region. From cell type annotations, most proteins were "Undefined"; i.e., expressed by multiple cell types or unknown. Among annotated proteins, neuronal proteins were most commonly altered in the midbrain dorsal raphe (11/13), medullary raphe (30/35), and the ventrolateral medulla (7/10).

We compared these SUDC cases to control cases in the frontal cortex and hippocampus [44]. An additional analysis of the SUDC cases in these brain regions when comparing SUDC-FS and SUDC-noFS identified altered proteins in frontal cortex (218 proteins), dentate gyrus (107), and hippocampal CA1-3 (51, $p < 0.05$, Supplementary Tables 8, 9, 10, Supplementary Fig. 1).

Signaling pathway analysis

In the midbrain dorsal raphe, the 178 altered proteins were associated with 90 signaling pathways (p value of overlap < 0.05; Supplementary Table 5); Fig. 2a shows the top 20 significant pathways. Most significantly, eukaryotic translation initiation was increased in SUDC-FS ($p = 3.09 \times 10^{-7}$, z = 1.00), in addition to other protein translation-related signaling pathways. Although TPH2 was detected (and similar in brainstem regions, Supplementary Tables 2,

Table 3 Top 20 significant proteins in midbrain dorsal raphe of SUDC-FS vs. SUDC-noFS

Gene ID	Protein name	UniProt ID	*p* value	Fold change
Increased				
DUSP3	Dual specificity protein phosphatase 3	P51452	1.88E−04	1.6
HNRNPF	Heterogeneous nuclear ribonucleoprotein F	P52597	1.96E−03	2.5
DIABLO	Diablo homolog, mitochondrial	Q9NR28	2.92E−03	1.6
TTR	Transthyretin	P02766	2.95E−03	3.1
VPS45	Vacuolar protein sorting-associated protein 45	Q9NRW7	3.64E−03	15.0
RPS3	40S ribosomal protein S3	P23396	5.89E−03	1.3
NDUFB5	NADH dehydrogenase [ubiquinone] 1 beta subcomplex subunit 5, mitochondrial	O43674	5.92E−03	2.2
Decreased				
SOD1	Superoxide dismutase [Cu–Zn]	P00441	2.29E−04	1.7
TSTA3	GDP-L-fucose synthase	Q13630	1.47E−03	1.3
SYNGR3	Synaptogyrin-3	O43761	2.23E−03	1.6
PRRT3	Proline-rich transmembrane protein 3	Q5FWE3	2.31E−03	1.4
PARK7	Parkinson disease protein 7	Q99497	3.44E−03	1.4
MAP4K4	Mitogen-activated protein kinase kinase kinase kinase 4	O95819	3.74E−03	1.9
ANXA7	Annexin A7	P20073	3.77E−03	1.3
SLC2A13	Proton myo-inositol cotransporter	Q96QE2	3.97E−03	24.9
CLASP1	CLIP-associating protein 1	Q7Z460	4.39E−03	1.6
MAPT	Microtubule-associated protein tau	P10636	4.45E−03	1.5
TXN	Thioredoxin	P10599	4.56E−03	1.6
LSAMP	Limbic system-associated membrane protein	Q13449	5.04E−03	1.6
ISYNA1	Inositol-3-phosphate synthase 1	Q9NPH2	5.61E−03	1.7

Table 4 Top 20 significant proteins in medullary raphe of SUDC-FS vs. SUDC-noFS

Gene ID	Protein name	UniProt ID	*p* value	Fold change
Increased				
RPS8	40S ribosomal protein S8	P62241	1.74E−05	1.3
PHB	Prohibitin	P35232	4.12E−05	1.2
SEZ6L2	Seizure 6-like protein 2	Q6UXD5	4.75E−05	3.9
CCT7	T-complex protein 1 subunit eta	Q99832	1.44E−04	1.3
RACK1	Receptor of activated protein C kinase 1	P63244	1.47E−04	1.4
RPL28	60S ribosomal protein L28	P46779	2.71E−04	1.4
ERP44	Endoplasmic reticulum resident protein 44	Q9BS26	3.54E−04	1.3
RPL12	60S ribosomal protein L12	P30050	4.07E−04	1.4
PCCA	Propionyl-CoA carboxylase alpha chain, mitochondrial	P05165	5.33E−04	1.2
VAMP2	Vesicle-associated membrane protein 2	P63027	6.15E−04	1.7
CCT3	T-complex protein 1 subunit gamma	P49368	7.86E−04	1.1
ATP6V1D	V-type proton ATPase subunit D	Q9Y5K8	8.20E−04	1.2
FARSA	Phenylalanine–tRNA ligase alpha subunit	Q9Y285	8.52E−04	1.6
RPS11	40S ribosomal protein S11	P62280	9.14E−04	1.4
RPSA	40S ribosomal protein SA	P08865	1.16E−03	1.2
RPS19	40S ribosomal protein S19	P39019	1.31E−03	1.3
CCT8	T-complex protein 1 subunit theta	P50990	1.35E−03	1.1
RPL36	60S ribosomal protein L36	Q9Y3U8	1.37E−03	1.5
LMAN1	Protein ERGIC-53	P49257	1.38E−03	2.4
Decreased				
AGPAT1	1-acyl-sn-glycerol-3-phosphate acyltransferase alpha	Q99943	9.84E−04	2.1

Table 5 Top 20 significant proteins in ventrolateral medulla of SUDC-FS vs. SUDC-noFS

Gene ID	Protein name	UniProt ID	*p* value	Fold change
Increased				
GRHPR	Glyoxylate reductase/hydroxypyruvate reductase	Q9UBQ7	3.29E−04	1.2
COX6B1	Cytochrome c oxidase subunit 6B1	P14854	1.34E−03	1.6
FKBP1B	Peptidyl-prolyl cis–trans isomerase FKBP1B	P68106	4.19E−03	1.3
F2	Prothrombin	P00734	7.03E−03	1.4
TMOD1	Tropomodulin-1	P28289	7.06E−03	1.4
DNAJA4	DnaJ homolog subfamily A member 4	Q8WW22	9.00E−03	1.2
DNAJC11	DnaJ homolog subfamily C member 11	Q9NVH1	9.03E−03	1.2
Decreased				
SERPINA1	Alpha-1-antitrypsin	P01009	1.86E−03	1.5
PCP4L1	Purkinje cell protein 4-like protein 1	A6NKN8	2.25E−03	1.8
MARCKS	Myristoylated alanine-rich C-kinase substrate	P29966	4.47E−03	1.4
SNCA	Alpha-synuclein	P37840	5.75E−03	1.3
PKP1	Plakophilin-1	Q13835	6.85E−03	2.6
BLMH	Bleomycin hydrolase	Q13867	6.95E−03	1.3
RAB12	Ras-related protein Rab-12	Q6IQ22	7.63E−03	1.5
PKP4	Plakophilin-4	Q99569	8.01E−03	1.5
GAP43	Neuromodulin	P17677	9.42E−03	1.6
HPX	Hemopexin	P02790	1.03E−02	1.6
SAFB	Scaffold attachment factor B1	Q15424	1.18E−02	1.6
G3BP2	Ras GTPase-activating protein-binding protein 2	Q9UN86	1.19E−02	1.3
PARP1	Poly [ADP-ribose] polymerase 1	P09874	1.22E−02	1.4

3, 4), serotonin receptors were not detected in any brain region analyzed. Serotonin receptor signaling was not altered in SUDC-FS ($p = 1.36 \times 10^{-1}$, z = -− 0.82). Several inflammation-related pathways were associated with protein differences, increased most significantly in the SUDC-noFS versus SUDC-FS cohorts for granzyme A signaling ($p = 1.95 \times 10^{-5}$, z = − 0.82). Hypoxia may play a role in SUDC cases; HIF1A signaling was increased in SUDC-noFS ($p = 2.04 \times 10^{-2}$, z = − 0.45).

In the medullary raphe, the 344 altered proteins were associated with 201 signaling pathways (Supplementary Table 6); Fig. 2b shows the top 20 significant pathways. Most significantly, eukaryotic translation elongation was increased in SUDC-FS ($p = 6.31 \times 10^{-49}$, z = 6.01), in addition to other protein translation-related signaling pathways. Serotonin receptor signaling was not altered in SUDC-FS ($p = 7.59 \times 10^{-2}$, z = − 0.30). Several inflammation-related signaling pathways were associated with altered proteins most significantly with increased neutrophil degranulation in the SUDC-FS group ($p = 4.07 \times 10^{-7}$, z = 1.04) and increased acute phase response in the SUDC-noFS group ($p = 1.38 \times 10^{-3}$, z = − 2.65). HIF1A signaling was increased in SUDC-noFS ($p = 5.37 \times 10^{-5}$, z = − 0.58).

In the ventrolateral medulla, the 100 altered proteins were associated with 82 signaling pathways (Supplementary Table 7), and the top 20 significant pathways are depicted in Fig. 2c. Most significantly, coagulation system was increased in SUDC-FS ($p = 1.32 \times 10^{-5}$, z = 1.00). Serotonin receptor signaling was mildly increased in SUDC-FS ($p = 4.57 \times 10^{-2}$, z = 0.44). Several inflammation-related pathways were associated with altered proteins, particularly within the SUDC-noFS group most significantly for neutrophil degranulation ($p = 2.82 \times 10^{-5}$, z = 0.00), and increased acute phase response in the SUDC-noFS group ($p = 1.20 \times 10^{-4}$, z = − 1.00). HIF1A signaling was mildly altered ($p = 5.75 \times 10^{-2}$, z = NA).

Compared to other brain regions [44], signaling pathways associated with altered proteins in SUDC-FS versus SUDC-noFS were identified (Supplementary Fig. 1, Supplementary Tables 11, 12, 13). Top significant pathways included selenoamino acid metabolism decreased in SUDC-FS frontal cortex ($p = 3.47 \times 10^{-9}$, z = -− 3.32), mitochondrial dysfunction increased in SUDC-FS dentate gyrus ($p = 4.27 \times 10^{-8}$, z = 2.11), and Gene and protein expression by JAK-STAT signaling after IL-12 stimulation mildly altered in the hippocampal CA1-3 ($p = 6.61 \times 10^{-5}$, z = NA). Serotonin receptor signaling was decreased in frontal cortex ($p = 1.02 \times 10^{-2}$, z = − 1.90), and not different in dentate gyrus ($p = 5.75 \times 10^{-2}$, z = − 1.34) or hippocampal CA1-3 ($p = 6.32 \times 10^{-1}$, z = NA). Several inflammation-related pathways were associated with protein differences including increased neutrophil degranulation in SUDC-noFS

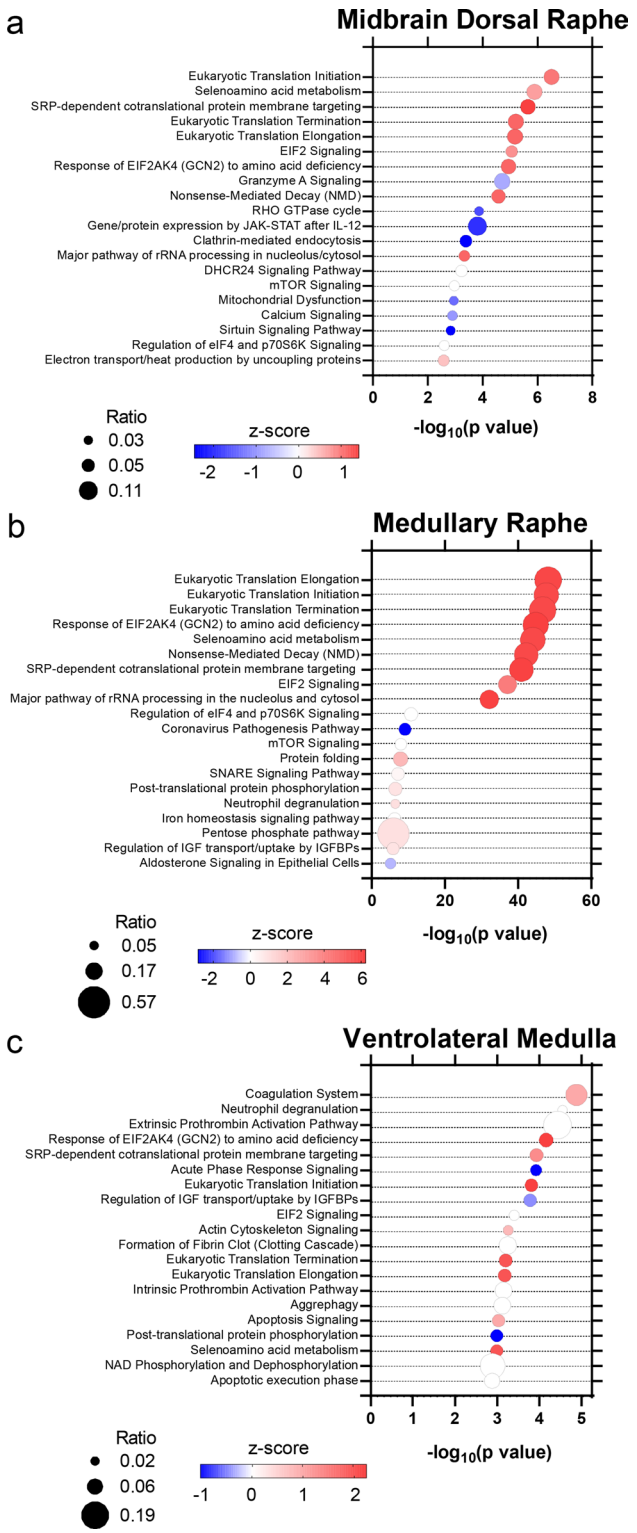

Fig. 2 Signaling pathways associated with differentially expressed proteins in the brainstem. **a** in the midbrain dorsal raphe, 90 signaling pathways (p value of overlap < 0.05) were associated with the altered proteins, **b** in the medullary raphe, 201 signaling pathways were associated with the altered proteins, **c** in the ventrolateral medulla, 82 signaling pathways were associated with altered proteins. The top 20 significant signaling pathways are depicted. Color indicates z-score, with red increased and blue decreased. The ratio of proteins altered in a pathway are indicated by circle size

frontal cortex ($p = 6.92 \times 10^{-8}$; z = − 4.36), increased neutrophil extracellular trap signaling pathway in SUDC-noFS in dentate gyrus ($p = 4.07 \times 10^{-4}$, z = − 2.12), and mildly altered neutrophil degranulation in the hippocampal CA1-3 ($p = 4.79 \times 10^{-4}$, z = − 0.82). In the frontal cortex, there was increased HIF1A signaling in SUDC-noFS ($p = 2.9 \times 10^{-3}$, z = -− 1.13) as well as cellular response to hypoxia ($p = 4.7 \times 10^{-3}$, z = − 1.00, Supplementary Table 11). HIF1A signaling was not altered in the two hippocampal regions evaluated (Supplementary Tables 12, 13).

When comparing all six brain regions evaluated by FS history, 62 signaling pathways were altered in ≥ 2 brain regions with at least one region impacted by fold-change as reflected by z-score (Fig. 3). Among the 62 pathways, three pathways were altered in five brain regions: neutrophil degranulation, synaptogenesis signaling pathway, and RHO GTPase cycle.

Brain region comparative analyses

Among significantly altered proteins in each brainstem region, there was no overlap of proteins in all three regions analyzed and some overlap when comparing two brain regions (Supplementary Fig. 2a). When comparing significantly altered proteins in at least one region, there was a poor negative correlation in the midbrain dorsal raphe and medullary raphe ($p = 0.0077$, $R^2 = 0.014$; Fig. 2b). Most proteins (60%; 294/493) were changing in different fold-change directions, and 40% of proteins (199/493) were changing in the same direction. There was no correlation of protein levels between the midbrain dorsal raphe and ventrolateral medulla ($p = 0.40$, $R^2 = 0.0027$; Supplementary Fig. 2c). There were 56% (154/273) of proteins changing in the same fold-change direction, and 44% (119/273) of proteins in the opposite direction. When comparing the medullary raphe and ventrolateral medulla, there was a poor positive correlation ($p < 0.0001$, $R^2 = 0.062$; Supplementary Fig. 2d). There were 65% (274/421) of proteins changing in the same fold-change direction, and 35% (147/421) of proteins changing in the opposite direction.

When comparing each brainstem region to previously analyzed frontal cortex and hippocampus, there were poor correlations or no correlations between all brain regions (Supplementary Fig. 3). These poor correlations reflect brain region specific protein expression and unique protein changes by region associated with FS history.

Immunofluorescent analyses

Top candidate proteins were evaluated by IF from among the most significantly altered proteins identified by proteomics, as well as the serotonin receptors 5HT1A and 5HT2A that

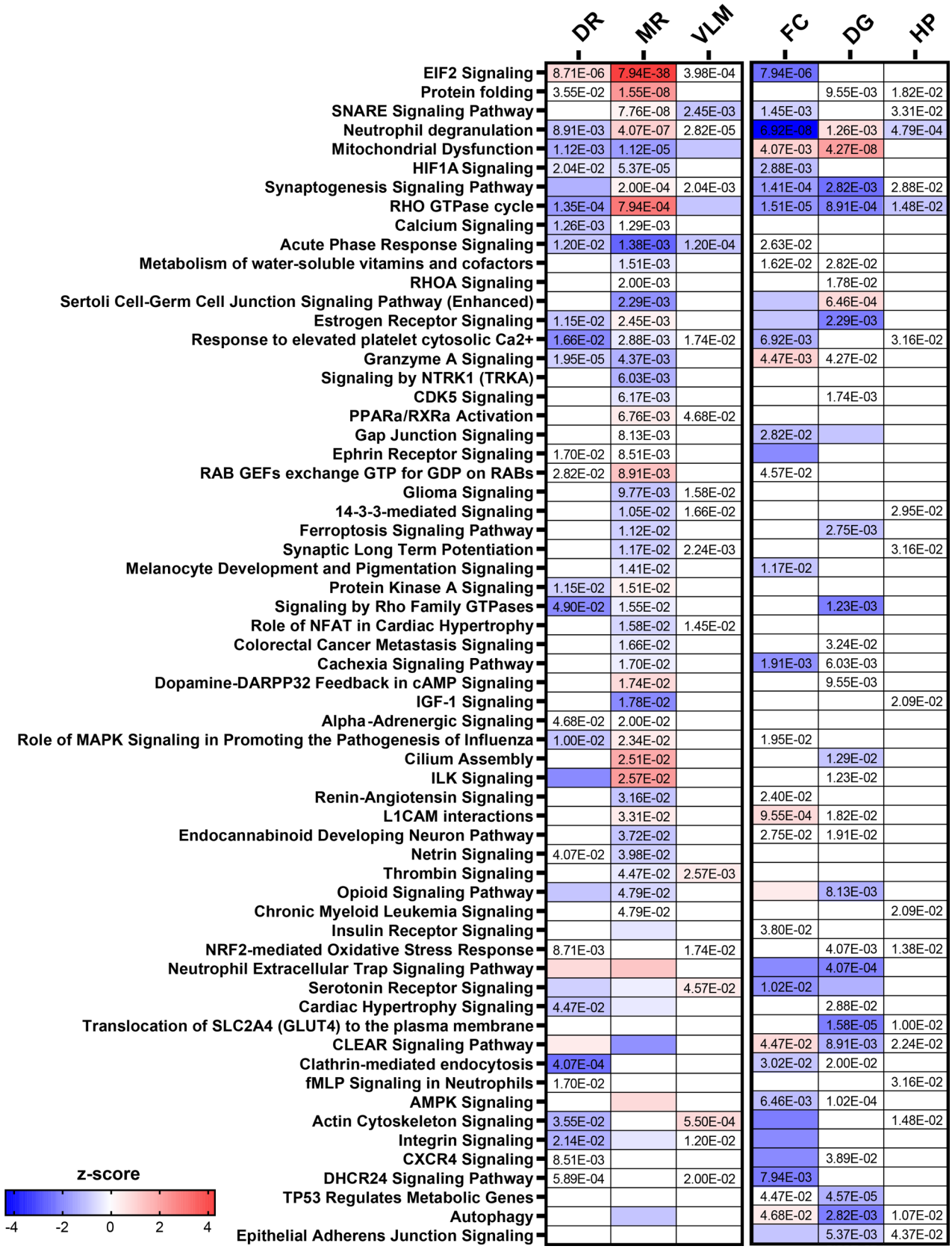
DR
MR
VLM
FC
DG
HP
EIF2 Signaling 8.71E-06 7.94E-38 3.98E-04 7.94E-06
Protein folding 3.55E-02 1.55E-08 9.55E-03 1.82E-02
SNARE Signaling Pathway 7.76E-08 2.45E-03 1.45E-03 3.31E-02
Neutrophil degranulation 8.91E-03 4.07E-07 2.82E-05 6.92E-08 1.26E-03 4.79E-04
Mitochondrial Dysfunction 1.12E-03 1.12E-05 4.07E-03 4.27E-08
HIF1A Signaling 2.04E-02 5.37E-05 2.88E-03
Synaptogenesis Signaling Pathway 2.00E-04 2.04E-03 1.41E-04 2.82E-03 2.88E-02
RHO GTPase cycle 1.35E-04 7.94E-04 1.51E-05 8.91E-04 1.48E-02
Calcium Signaling 1.26E-03 1.29E-03
Acute Phase Response Signaling 1.20E-02 1.38E-03 1.20E-04 2.63E-02
Metabolism of water-soluble vitamins and cofactors 1.51E-03 1.62E-02 2.82E-02
RHOA Signaling 2.00E-03 1.78E-02
Sertoli Cell-Germ Cell Junction Signaling Pathway (Enhanced) 2.29E-03 6.46E-04
Estrogen Receptor Signaling 1.15E-02 2.45E-03 2.29E-03
Response to elevated platelet cytosolic Ca2+ 1.66E-02 2.88E-03 1.74E-02 6.92E-03 3.16E-02
Granzyme A Signaling 1.95E-05 4.37E-03 4.47E-03 4.27E-02
Signaling by NTRK1 (TRKA) 6.03E-03
CDK5 Signaling 6.17E-03 1.74E-03
PPARa/RXRa Activation 6.76E-03 4.68E-02
Gap Junction Signaling 8.13E-03 2.82E-02
Ephrin Receptor Signaling 1.70E-02 8.51E-03
RAB GEFs exchange GTP for GDP on RABs 2.82E-02 8.91E-03 4.57E-02
Glioma Signaling 9.77E-03 1.58E-02
14-3-3-mediated Signaling 1.05E-02 1.66E-02 2.95E-02
Ferroptosis Signaling Pathway 1.12E-02 2.75E-03
Synaptic Long Term Potentiation 1.17E-02 2.24E-03 3.16E-02
Melanocyte Development and Pigmentation Signaling 1.41E-02 1.17E-02
Protein Kinase A Signaling 1.15E-02 1.51E-02
Signaling by Rho Family GTPases 4.90E-02 1.55E-02 1.23E-03
Role of NFAT in Cardiac Hypertrophy 1.58E-02 1.45E-02
Colorectal Cancer Metastasis Signaling 1.66E-02 3.24E-02
Cachexia Signaling Pathway 1.70E-02 1.91E-03 6.03E-03
Dopamine-DARPP32 Feedback in cAMP Signaling 1.74E-02 9.55E-03
IGF-1 Signaling 1.78E-02 2.09E-02
Alpha-Adrenergic Signaling 4.68E-02 2.00E-02
Role of MAPK Signaling in Promoting the Pathogenesis of Influenza 1.00E-02 2.34E-02 1.95E-02
Cilium Assembly 2.51E-02 1.29E-02
ILK Signaling 2.57E-02 1.23E-02
Renin-Angiotensin Signaling 3.16E-02 2.40E-02
L1CAM interactions 3.31E-02 9.55E-04 1.82E-02
Endocannabinoid Developing Neuron Pathway 3.72E-02 2.75E-02 1.91E-02
Netrin Signaling 4.07E-02 3.98E-02
Thrombin Signaling 4.47E-02 2.57E-03
Opioid Signaling Pathway 4.79E-02 8.13E-03
Chronic Myeloid Leukemia Signaling 4.79E-02 2.09E-02
Insulin Receptor Signaling 3.80E-02
NRF2-mediated Oxidative Stress Response 8.71E-03 1.74E-02 4.07E-03 1.38E-02
Neutrophil Extracellular Trap Signaling Pathway 4.07E-04
Serotonin Receptor Signaling 4.57E-02 1.02E-02
Cardiac Hypertrophy Signaling 4.47E-02 2.88E-02
Translocation of SLC2A4 (GLUT4) to the plasma membrane 1.58E-05 1.00E-02
CLEAR Signaling Pathway 4.47E-02 8.91E-03 2.24E-02
Clathrin-mediated endocytosis 4.07E-04 3.02E-02 2.00E-02
fMLP Signaling in Neutrophils 1.70E-02 3.16E-02
AMPK Signaling 6.46E-03 1.02E-04
Actin Cytoskeleton Signaling 3.55E-02 5.50E-04 1.48E-02
Integrin Signaling 2.14E-02 1.20E-02
CXCR4 Signaling 8.51E-03 3.89E-02
DHCR24 Signaling Pathway 5.89E-04 2.00E-02 7.94E-03
TP53 Regulates Metabolic Genes 4.47E-02 4.57E-05
Autophagy 4.68E-02 2.82E-03 1.07E-02
Epithelial Adherens Junction Signaling 5.37E-03 4.37E-02
z-score
-4 -2 0 2 4

◂**Fig. 3** Signaling pathways altered in multiple brain regions. Among the six brain regions (DR = dorsal raphe, MR = medullary raphe, VLM = ventrolateral medulla, FC = frontal cortex, DG = dentate gyrus, HP = hippocampal CA1-3) evaluated in SUDC, there were 62 signaling pathways that were significantly altered in at least 2 brain regions (*p* value) and impacted by fold-change in at least one brain region (z-score). Pathways are sorted by most significant in the medullary raphe. Z-score is indicated by color, increased (red), decreased (blue). *P* value of overlap is indicated for the signaling pathways at $p < 0.05$

are implicated in SIDS and SUDEP [31, 33, 38] and thus may play a role in SUDC.

Tables 3, 4, 5 show the proteins with the highest fold-change included SLC2A13 in the midbrain dorsal raphe and SEZ6L2 in the medullary raphe. SLC2A13 (also known as HMIT, proton H + myo-inositol symporter) was decreased 24.9-fold in SUDC-FS by proteomics ($p = 3.97 \times 10^{-3}$), which showed a similar trend by IF from percent positive area with a 1.5-fold decrease in the midbrain dorsal raphe ($p = 0.23$, Fig. 4). SEZ6L2 (Seizure Related 6 Homolog Like 2, also known as BSRP-A brain specific receptor-like proteins-A) was increased 3.9-fold in SUDC-FS by proteomics ($p = 4.75 \times 10^{-5}$), which showed a similar trend by IF from percent positive area with a 1.3-fold increase ($p = 0.49$, Fig. 4). SLC2A13 and SEZ6L2 were present in some TPH2(+) cells, as well as in other neighboring TPH2(−) cells. Colocalization analyses showed a moderate correlation by Mander coefficient of TPH2 (green channel) to SLC2A13 (red channel), with a lower correlation identified in the SUDC-FS group when compared to the SUDC-noFS group ($p = 0.026$; Fig. 4d). This reflects the lower level of SLC2A13 in SUDC-FS, which is present predominantly in TPH2(+) cells. For SEZ6L2, colocalization analyses showed no difference between SUDC-FS and SUDC-noFS in either channel.

Serotonin receptors 5HT1A and 5HT2A were evaluated by IF in the brainstem regions of interest. These proteins were not detected by proteomics but may play a role in SUDC. In the midbrain dorsal raphe, 5HT1A ($p = 0.77$) and 5HT2A ($p = 0.29$) were not different when comparing SUDC-FS and SUDC-noFS (Fig. 5). In the medullary raphe, 5HT2A ($p = 0.025$) was 2.1-fold increased in SUDC-FS, while 5HT1A ($p = 0.83$) was not different (Fig. 6). In the ventrolateral medulla, 5HT1A ($p = 0.53$) and 5HT2A ($p = 0.29$) were not different (Fig. 7). Variability was observed within groups, which may reflect the level of the brainstem sampled, protein specific changes in the region, and heterogeneity of case history and mechanisms of death. In all brain regions, both 5HT1A and 5HT2A receptors were present in TPH2(+) cells or other neighboring TPH2(−) cells as has been previously observed [6, 7, 35, 54, 55] and colocalization did not differ by FS history (Figs. 5, 6, 7). There was less colocalization of 5HT2A and TPH2 in all brainstem regions, as reflected by a lower correlation or no correlation by Mander coefficient. TPH2 was not different by proteomics or by IF in any brainstem region analyzed (Supplementary Tables 2, 3, 4, Figs. 4, 5, 6, 7).

Correlation to clinical history

To identify proteins that may correlate with clinical features, a WGCNA was performed in each brain region (Fig. 8, Supplementary Fig. 4, Supplementary Tables 14, 15, 16). The most significant protein clusters identified were correlated to FS history duration, which was most significantly correlated to protein levels in the ventrolateral medulla as well as in the medullary raphe. In the ventrolateral medulla, the most significantly correlated protein cluster was associated with FS history duration ($p = 1.60 \times 10^{-7}$, corr = − 0.90) and was related to decreased synaptic vesicle cycle from the top GO BP term (FDR < 5% with at least 5 proteins, Supplementary Table 16). In the medullary raphe, the most significantly correlated protein cluster was associated with FS history duration ($p = 9.80 \times 10^{-5}$, corr = − 0.80) and was associated with decreased aerobic respiration (Supplementary Table 15). Serotonin receptor (5HT1A and 5HT2A) IF levels were assessed for correlation to protein clusters. Fifteen protein clusters correlated to serotonin receptor levels, and one cluster with a significant GO BP term in the medullary raphe related the higher 5HT2A levels with higher extracellular matrix organization proteins ($p = 3.93 \times 10^{-2}$, corr = − 0.50). The midbrain dorsal raphe had fewer modules associated significantly with case history (Supplementary Table 14). From the previously analyzed brain regions, case history had fewer correlations with GO BP terms (Supplementary Figs. 5, 6, Supplementary Tables 17, 18, 19).

Discussion

We identified protein differences in brainstem regions when comparing SUDC cases with FS versus those without FS, particularly in the medullary raphe. The most robust protein differences were associated with increased protein translation-related signaling pathways in the medullary raphe and to a lesser extent in the midbrain dorsal raphe. The serotonin receptor 5HT2A was increased in the medullary raphe histologically. In SUDC-noFS cases, there was increased inflammation-related and HIF1A signaling pathways in the brainstem relative to the SUDC-FS cases. Overall, protein differences in SUDC were identified in brain regions related to respiratory function and arousal.

The medullary raphe had the most protein differences identified in SUDC-FS across the six brain regions analyzed, most significantly associated with increased protein translation-related signaling pathways. Increased protein

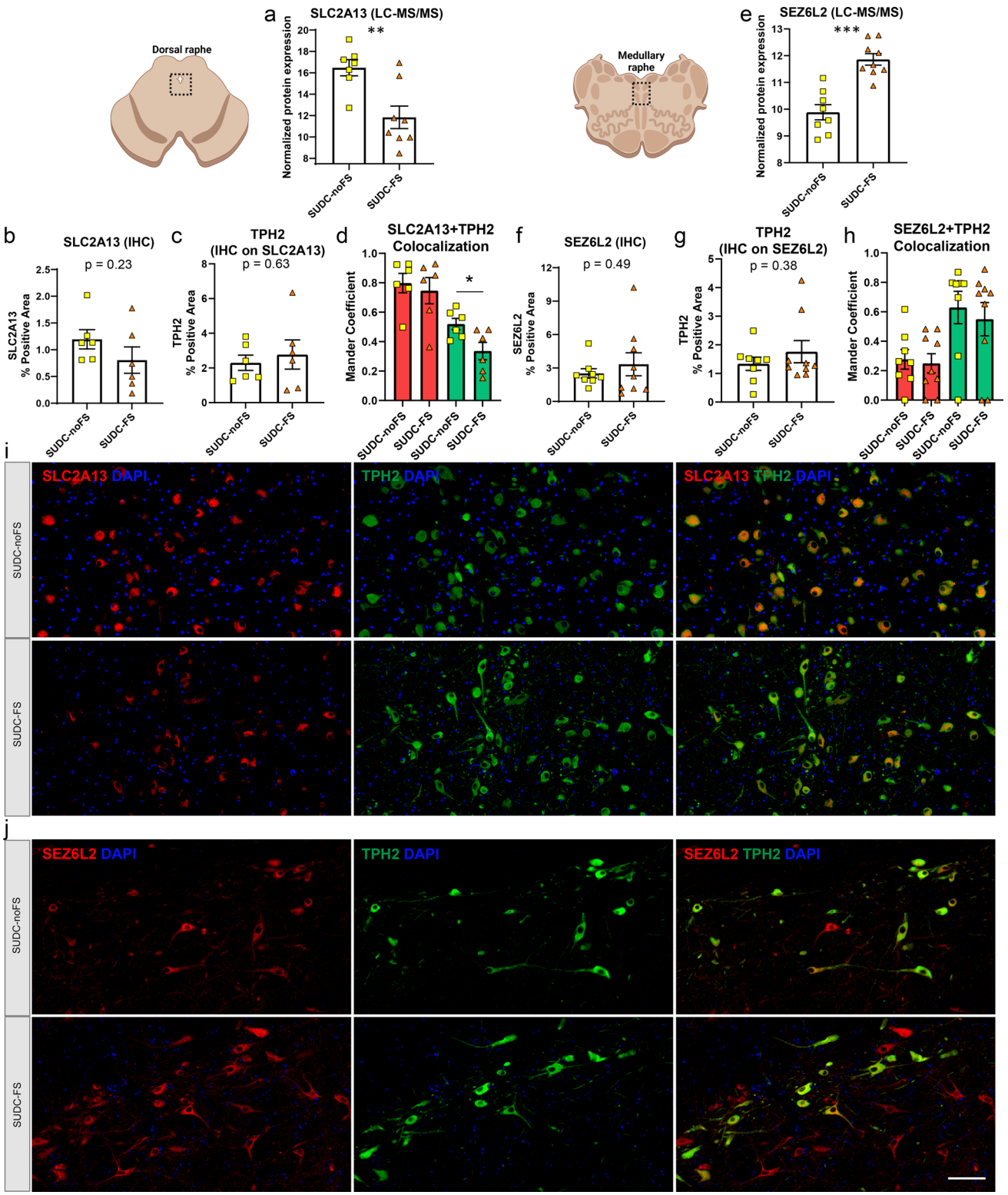

translation-related signaling pathways were observed to a lesser extent in the midbrain dorsal raphe, decreased in the frontal cortex, and not altered in hippocampus. There was strong enrichment for many ribosome proteins among the protein translation-related signaling pathways in SUDC-FS, and the increases were typically less than two-fold in the medullary raphe relative to SUDC-noFS. Our previous study [44] is the only human SUDC-FS brain tissue proteomic analysis. Altered ribosomal function has been associated with seizures [21, 26, 74], cell

◂**Fig. 4** Histological localization and quantification of top protein candidates SLC2A13 and SEZ6L2 in the brainstem. **a** By LC–MS/MS in the midbrain dorsal raphe, SLC2A13 was among the top significant proteins and had the largest fold change with a 24.9-fold decrease in SUDC-FS when compared to SUDC-noFS ($p = 3.97 \times 10^{-3}$), **b** IF for SLC2A13 in the midbrain dorsal raphe showed a similar trend with a 1.5-fold decrease in SUDC-FS ($p = 0.23$) from semiquantitative analysis, **c** IF for TPH2 on the same slides for SLC2A13 in the midbrain dorsal raphe showed no difference between SUDC-FS and SUDC-noFS, similar to proteomics, **d** colocalization analysis of SLC2A13 and TPH2 in the midbrain dorsal raphe showed a moderate correlation by Mander coefficient of the green channel (TPH2), which was different between SUDC-FS and SUDC-noFS ($p = 0.026$). There was a higher correlation in the red channel (SLC2A13) for both SUDC-FS and SUDC-noFS. **e** By LC–MS/MS in the medullary raphe, SEZ6L2 was among the top significant proteins and had the largest fold change with a 3.9-fold increase in SUDC-FS ($p = 4.75 \times 10^{-5}$), **f** IF for SEZ6L2 in the medullary raphe showed a similar trend with a 1.3-fold increase ($p = 0.49$) from semiquantitative analysis, **g** IF for TPH2 on the same slides for SEZ6L2 in the medullary raphe showed no difference between SUDC-FS and SUDC-noFS, similar to proteomics, **h** colocalization analysis of SEZ6L2 and TPH2 in the medullary raphe showed a low correlation in the red channel and moderate correlation in the green channel, which was not different between SUDC-FS and SUDC-noFS, **i** representative images from IF in the midbrain dorsal raphe are shown for SLC2A13 (red) and TPH2 (green) in SUDC-FS and SUDC-noFS. TPH2 indicates the region with serotonergic neurons that was microdissected for proteomic analysis. SLC2A13 was present in TPH2(+) cells, as well as in other neighboring TPH2(−) cells, **j** representative images from IF in the medullary raphe are shown for SEZ6L2 (red) and TPH2 (green) in SUDC-FS and SUDC-noFS. TPH2 indicates the region with serotonergic neurons that was microdissected for proteomic analysis. SEZ6L2 was present in TPH2(+) cells, as well as in other neighboring TPH2(−) cells. Scale bar 100 um. Error bars indicate SEM

stress response influenced ribosome protein levels [58, 62]. We observed increased protein translation-related proteins in epilepsy from the hippocampal CA1-3 region [37, 59] but not brainstem [43]. Altered ribosome function may remodel the local proteome [10] and influence neuronal growth and synaptic plasticity that could contribute to epileptogenesis in hippocampus and forebrain of chronic animal epilepsy models [74]. Thus, our results in SUDC-FS identified differences in translation proteins in the brainstem and frontal cortex, but not in the hippocampus of these same cases, differently than is seen in adult epilepsy [43, 59]. To better define how these proteomic differences may relate to SUDC mechanisms of death, it will be of interest to evaluate whether these medullary protein translation-related signaling pathways can be a protective compensatory response or whether these protein differences are associated with increased risk for dysregulation. These protein translation-related proteins should be characterized further in future mechanistic studies to understand how these protein differences relate to the many other protein differences observed in this brain region, particularly including those proteins related to the chemosensitive respiratory response in the medullary raphe may be critical.

Serotonergic related dysfunction may occur in SUID/SIDS and SUDEP [12, 38, 57, 77], thus may be involved in SUDC. In our study, serotonin 5HT2A receptor was increased in the medullary raphe histologically, and serotonin receptor signaling was mildly altered in two brain regions as detected by proteomics (increased ventrolateral medulla, decreased frontal cortex). Further, there was variability in the serotonin receptor expression levels that may reflect group heterogeneity, including high perivascular 5HT2A observed in the midbrain dorsal raphe of one SUDC-noFS case. 5HT2A is expressed by multiple cell types in the brain, including neurons, glia, and in cell types of the vasculature [5, 46, 49]. We previously identified increased 5HT2A levels in resected hippocampus from epilepsy patients, with a positive correlation to prolonged postictal generalized EEG suppression (PGES) that is associated with increased SUDEP risk [38]. Serotonin receptors influence seizure activity, arousal response, respiratory function, and 5HT2A antagonists decrease seizure frequency in animal models [3, 15, 18, 73]. The functional implications and associations of increased medullary 5HT2A with SUDC risk should be evaluated further.

From our brainstem proteomics results, two top protein candidates, SLC2A13 and SEZ6L2, were identified in association with FS. In the midbrain dorsal raphe, SLC2A13 was 24.9-fold decreased in SUDC-FS. This protein was decreased 11.5-fold in the medullary raphe, but not different in the ventrolateral medulla, and not detected in the frontal cortex or hippocampal regions. By IF, SLC2A13 was predominantly localized in TPH2(+) cells and was at a lower level in SUDC-FS cases in the midbrain dorsal raphe. We previously found a small increase in this protein in frontal cortex but not in hippocampus when comparing epilepsy and control cases [43, 59]. SLC2A13 is involved in exocytosis at synapses and growth cones [72], and it is a gamma-secretase associated protein that positively regulates amyloid beta production [68]. In the medullary raphe, SEZ6L2 was 3.9-fold increased in SUDC-FS. This protein was not different in other brain regions, nor in epilepsy or SUDEP brain regions [43, 59]. Physiological functions of SEZ6L2 may include a role in neuronal differentiation with secreted soluble forms of SEZ6L2 produced via cathepsin D, and modulation of AMPA receptors by binding to glutamate receptor 1 and adducin [8, 75]. Triple knockout mouse models of the *SEZ6* family members (*SEZ6*/*SEZ6L*/*SEZ6L2*) have decreased protein kinase C phosphorylation and motor dysfunction [50]; knockout mouse models of *SEZ6* increased seizure threshold [19]. Decreased or disrupted SEZ6L2 protein levels by autoantibodies were associated with paraneoplastic cerebellar ataxia [14, 29], genetic variants in the *SEZ6* gene family may be associated with febrile seizures [52], and SEZ6L2

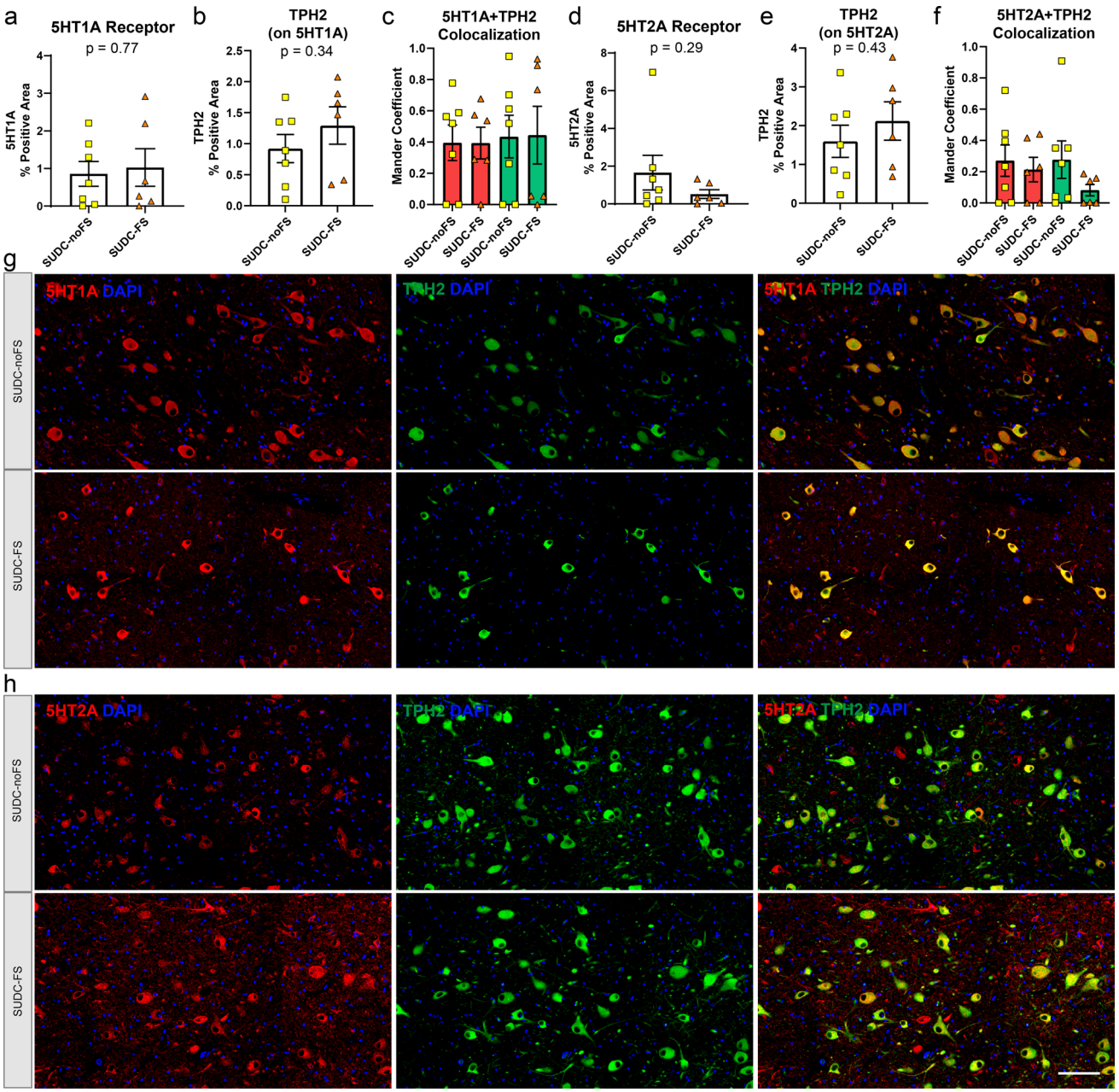

Fig. 5 Serotonin 5HT1A and 5HT2A receptor histological localization and quantification in the midbrain dorsal raphe. From IHC semi-quantitative analysis, there was no difference in **a** serotonin receptor 5HT1A ($p=0.77$) when comparing SUDC-FS and SUDC-noFS, **b** TPH2 from IF on the same tissue sections with 5HT1A was evaluated in colocalization analyses, **c** colocalization analysis of 5HT1A and TPH2 showed a moderate correlation by Mander coefficient of the red and green channels, with no difference between SUDC-FS and SUDC-noFS, **d** there was no difference in serotonin receptor 5HT2A ($p=0.29$) when comparing SUDC-FS and SUDC-noFS, **e** TPH2 from IF on the same tissue sections with 5HT2A was evaluated in colocalization analyses, **f** colocalization analysis of 5HT2A and TPH2 showed lower correlations in the red and green channels, with no difference between SUDC-FS and SUDC-noFS. Representative images from IF are shown for 5HT1A (red) **g**, 5HT2A (red) **h**, and TPH2 (green) in SUDC-FS and SUDC-noFS. TPH2 indicates the region with serotonergic neurons that was microdissected for proteomic analysis. Scale bar 100 um. Error bars indicate SEM

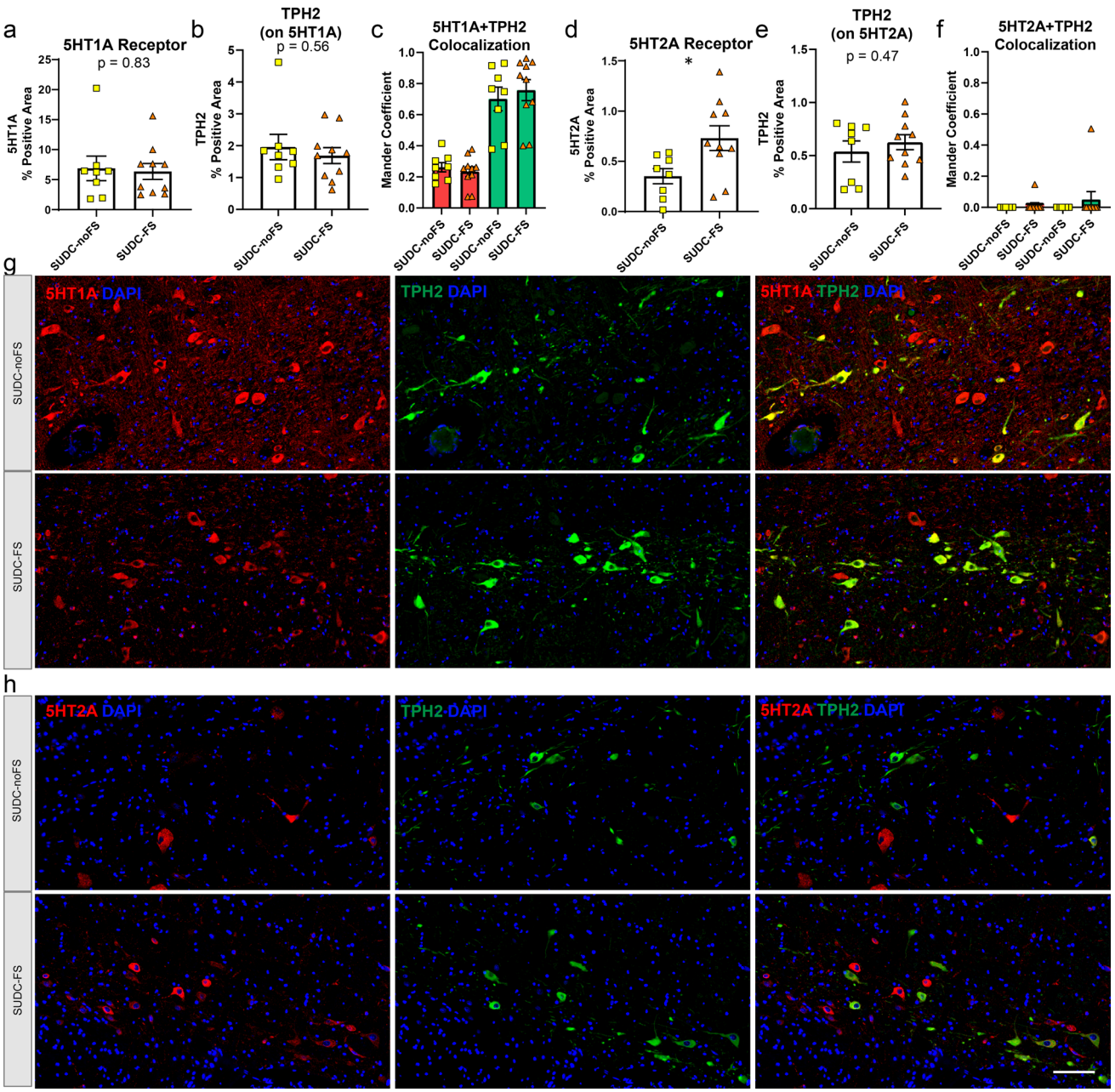

Fig. 6 Serotonin 5HT1A and 5HT2A receptor histological localization and quantification in the medullary raphe. From IF semiquantitative analysis, there was no difference in **a** serotonin receptor 5HT1A ($p=0.83$) when comparing SUDC-FS and SUDC-noFS, **b** TPH2 from IF on the same tissue sections with 5HT1A was evaluated in colocalization analyses, **c** colocalization analysis of 5HT1A and TPH2 showed a low correlation by Mander coefficient in the red channel and a moderate correlation in the green channel, with no difference between SUDC-FS and SUDC-noFS **d** serotonin receptor 5HT2A was 2.1-fold increased ($p=0.025$) when comparing SUDC-FS and SUDC-noFS, **e** TPH2 from IF on the same tissue sections with 5HT2A was evaluated in colocalization analyses, **f** colocalization analysis of 5HT2A and TPH2 showed no correlation of the red and green channels. Representative images from IF are shown for 5HT1A (red) **g**, 5HT2A (red) **h**, and TPH2 (green) in SUDC-FS and SUDC-noFS. TPH2 indicates the region with serotonergic neurons that was microdissected for proteomic analysis. Scale bar 100 um. Error bars indicate SEM

was proposed as a CSF biomarker distinguishing idiopathic normal pressure hydrocephalus from Alzheimer's disease [70]. It will be of interest to further characterize SLC2A13 and SEZ6L2 in the context of development, FS, respiration regulation, and SUDC risk, including follow up mechanistic studies and whether increased SEZ6L2 brain, CSF, or neuron derived plasma levels may function as a biomarker of FS.

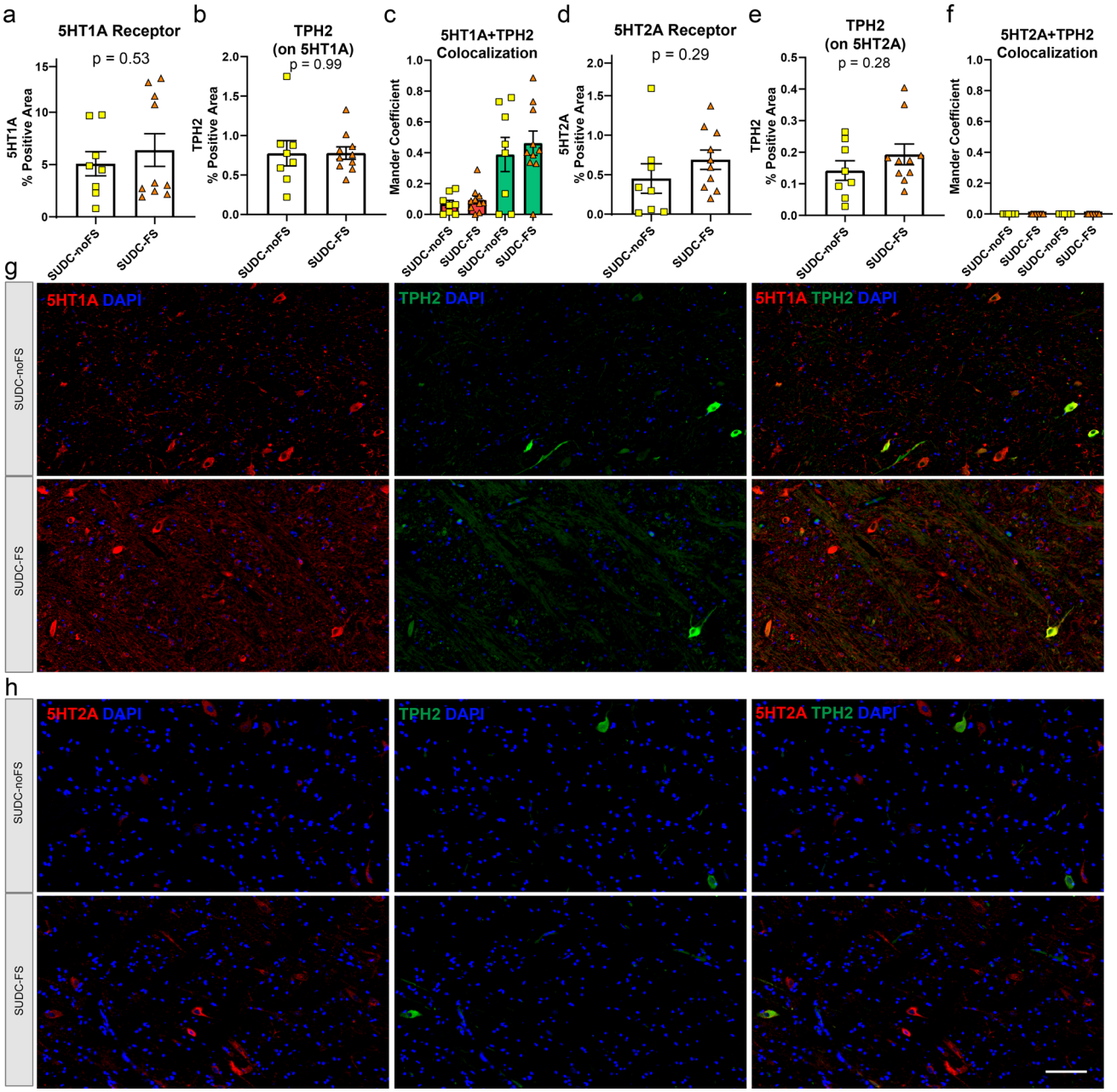

Fig. 7 Serotonin 5HT1A and 5HT2A receptor histological localization and quantification in the ventrolateral medulla. From IF semi-quantitative analysis, there was no difference in **a** serotonin receptor 5HT1A ($p=0.53$) when comparing SUDC-FS and SUDC-noFS, **b** TPH2 from IF on the same tissue sections with 5HT1A was evaluated in colocalization analyses, **c** colocalization analysis of 5HT1A and TPH2 showed a low correlation by Mander coefficient in the red channel and a moderate correlation in the green channel, with no difference between SUDC-FS and SUDC-noFS, **d** There was no difference in serotonin receptor 5HT2A ($p=0.29$) when comparing SUDC-FS and SUDC-noFS, **e** TPH2 from IF on the same tissue sections with 5HT2A was evaluated in colocalization analyses, **f** colocalization analysis of 5HT2A and TPH2 showed no correlation of the red and green channels. Representative images from IHC are shown for 5HT1A (red) **g**, 5HT2A (red) **h**, and TPH2 (green) in SUDC-FS and SUDC-noFS. Scale bar 100 um. Error bars indicate SEM

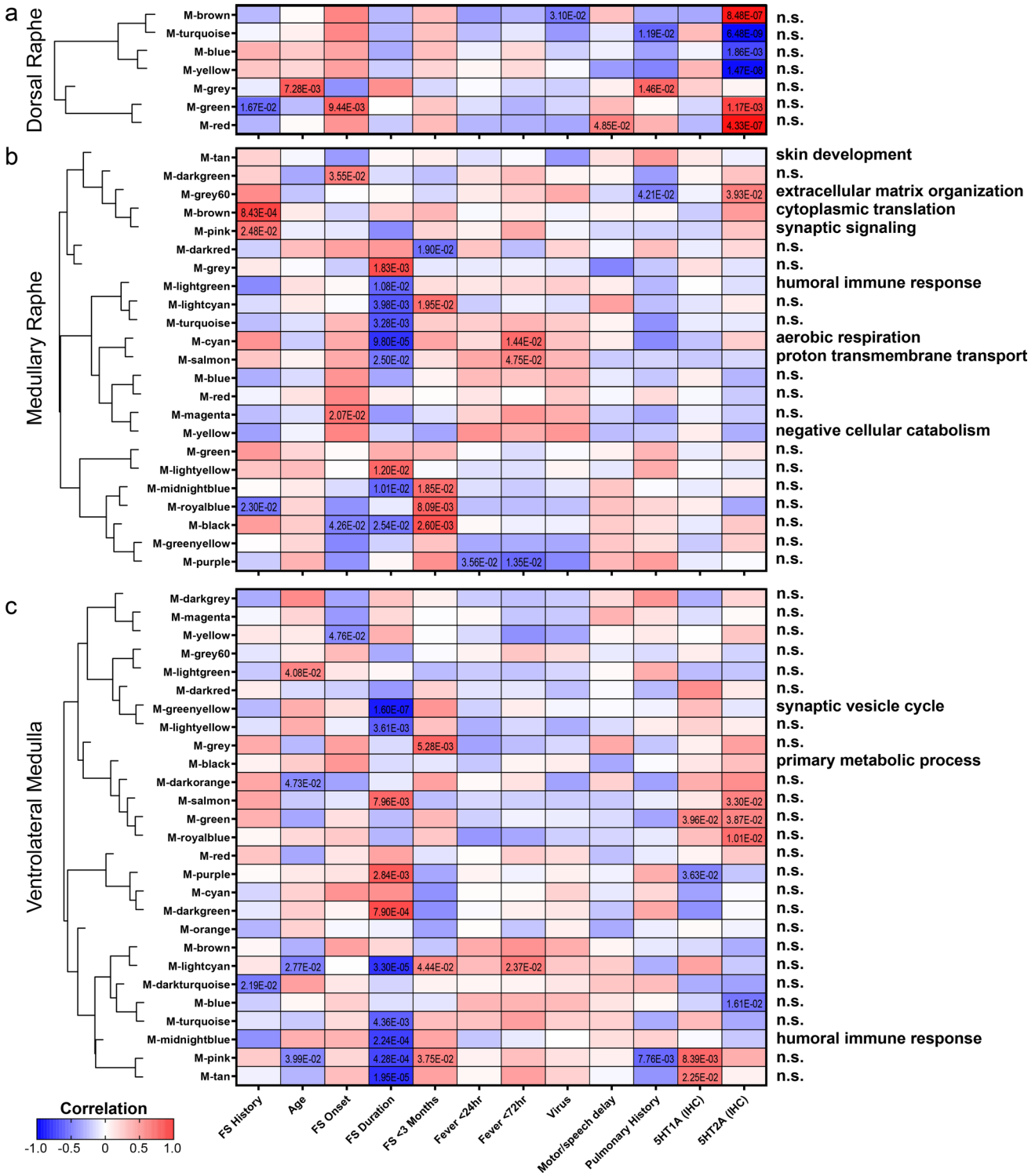

Fig. 8 WGCNA of case history in midbrain dorsal raphe, medullary raphe, and the ventrolateral medulla. A correlation analysis of case history variables to proteomics indicated significant modules and associated GO BP annotations in the **a** midbrain dorsal raphe, **b** medullary raphe, and **c** ventrolateral medulla. Modules are clustered by eigenprotein adjacency (relatedness to other modules) on the left. Name of module is indicated by "M-color" and corresponding color block. *P* values are indicated for those modules with $p < 0.05$ correlation. Positive correlation is indicated in red and negative correlation in blue. Top module GO BP annotations are noted on the right (FDR < 5% with at least 5 proteins) and detailed in Supplementary Tables 14, 15, 16. Several modules did not have a significant GO BP annotation and are noted as "n.s." = not significant. FS = febrile seizure. FS duration = FS history duration

FS history duration correlated significantly with protein expression levels in SUDC cases. Top correlated proteins with FS history duration were associated with a negative correlation to synaptic vesicle cycle proteins in the ventrolateral medulla and negative correlation to aerobic respiration in the medullary raphe. Common to both medullary regions was a negative correlation to humoral immune response in association with longer FS history duration. There was little to no correlation of protein levels and GO biological processes with other clinical features. Overall, the medulla showed strong associations with FS case history and should be evaluated further to determine how these findings may be associated with neurodevelopment and SUDC risk.

In SUDC-noFS, there were increased brainstem inflammation-related and HIF1A signaling pathways relative to SUDC-FS cases, which we observed in other brain regions in this study and compared to control cases [44]. In our previous epilepsy proteomic studies, these pathways were not altered in any brain region when comparing non-SUDEP epilepsy to SUDEP or control cases [40, 43, 59]. Thus, when comparing SUDC-noFS to SUDC-FS, there were protein differences associated with inflammatory processes and hypoxia signaling, particularly in the brainstem and frontal cortex but not in the hippocampus. Future studies should determine how these protein differences are associated with mechanisms of death in SUDC-noFS, including how protein differences vary in this potentially heterogeneous group.

There were some limitations in the study. Control cases with an explained cause of death did not have sufficient brainstem tissue available for comparison to SUDC cases and future studies should explore this group and FS cases with an explained COD. Some variability was observed within the SUDC groups, which may reflect variations in the level of the brainstem sample available, protein specific changes in the brain region related to case history, and heterogeneity of clinical features and related mechanisms of death. Further, cases were evaluated for known FS history, thus unwitnessed febrile seizure(s) that may occur as a terminal seizure during a sleep period may occur and also be associated with different protein changes [17], thus it is of interest to identify biomarkers of FS. Previous studies [31, 33] have included receptor binding and serotonin levels which were not assessed in this study. From the proteomic technique used, there can be lower or no detection of large membrane proteins and proteins with low abundance.

In conclusion, after evaluating six brain regions, most protein differences when comparing SUDC-FS and SUDC-noFS were in the medullary raphe and were related to a shift in protein translation-related signaling pathways. Further, serotonin 5HT2A receptor was increased in the medullary raphe. Future studies should assess whether these protein differences impair neurodevelopment and whether the result of FS history alters proteins further to increase SUDC risk.

Supplementary Information The online version contains supplementary material available at https://doi.org/10.1007/s00401-024-02832-9.

Acknowledgements We wish to thank the families, clinicians, medical examiners, and coroners for their participation in this research.

Author contributions LG, OD, and DL conceived and designed the study. DL, EK, and BU were responsible for analysis, immunohistochemistry, and figure generation. DL, CW, AF, EK, MS, DM, TW, BU, LG were responsible for data collection. DL, LG, and OD wrote the manuscript with input from co-authors. All authors read and approved the final manuscript.

Funding The research leading to these results has received funding from the Sudden Unexplained Death in Childhood (SUDC) Foundation, the Moss Pieratt Foundation, Emersyn Grace Rima Foundation, Finding A Cure for Epilepsy and Seizures at NYU (FACES), and by NIH grants P01AG060882 and P30AG066512.

Data availability All data are available in the supplementary data and in the online repository at the server (https://massive.ucsd.edu/) under accession MSV000095576.

Declarations

Conflict of interest The authors declare no competing interests.

References

1. Ackerman MJ, Andrew TA, Baker AM, Devinsky O, Downs JC, Keens T et al (2016) An association of hippocampal malformations and sudden death? We need more data. Forensic Sci Med Pathol 12:229–231. https://doi.org/10.1007/s12024-016-9765-1
2. Aira Z, Buesa I, Gallego M, García del Caño G, Mendiable N, Mingo J et al (2012) Time-dependent cross talk between spinal serotonin 5-HT2A receptor and mGluR1 subserves spinal hyperexcitability and neuropathic pain after nerve injury. J Neurosci 32:13568–13581. https://doi.org/10.1523/JNEUROSCI.1364-12.2012
3. Bagdy G, Kecskemeti V, Riba P, Jakus R (2007) Serotonin and epilepsy. J Neurochem 100:857–873. https://doi.org/10.1111/j.1471-4159.2006.04277.x

4. Benarroch EE (2014) Medullary serotonergic system: organization, effects, and clinical correlations. Neurology 83:1104–1111. https://doi.org/10.1212/WNL.0000000000000806
5. Berger M, Gray JA, Roth BL (2009) The expanded biology of serotonin. Annu Rev Med 60:355–366. https://doi.org/10.1146/annurev.med.60.042307.110802
6. Berry SA, Shah MC, Khan N, Roth BL (1996) Rapid agonist-induced internalization of the 5-hydroxytryptamine2A receptor occurs via the endosome pathway in vitro. Mol Pharmacol 50:306–313
7. Bhattacharyya S, Puri S, Miledi R, Panicker MM (2002) Internalization and recycling of 5-HT2A receptors activated by serotonin and protein kinase C-mediated mechanisms. Proc Natl Acad Sci U S A 99:14470–14475. https://doi.org/10.1073/pnas.212517999
8. Boonen M, Staudt C, Gilis F, Oorschot V, Klumperman J, Jadot M (2016) Cathepsin D and its newly identified transport receptor SEZ6L2 can modulate neurite outgrowth. J Cell Sci 129:557–568. https://doi.org/10.1242/jcs.179374
9. Crandall LG, Lee JH, Friedman D, Lear K, Maloney K, Pinckard JK et al (2020) Evaluation of concordance between original death certifications and an expert panel process in the determination of sudden unexplained death in childhood. JAMA Netw Open 3:e2023262. https://doi.org/10.1001/jamanetworkopen.2020.23262
10. Dastidar SG, Nair D (2022) A ribosomal perspective on neuronal local protein synthesis. Front Mol Neurosci 15:823135. https://doi.org/10.3389/fnmol.2022.823135
11. Devinsky O, Hesdorffer DC, Thurman DJ, Lhatoo S, Richerson G (2016) Sudden unexpected death in epilepsy: epidemiology, mechanisms, and prevention. Lancet Neurol 15:1075–1088. https://doi.org/10.1016/S1474-4422(16)30158-2
12. Duncan JR, Paterson DS, Hoffman JM, Mokler DJ, Borenstein NS, Belliveau RA et al (2010) Brainstem serotonergic deficiency in sudden infant death syndrome. JAMA 303:430–437. https://doi.org/10.1001/jama.2010.45
13. Dunn KW, Kamocka MM, McDonald JH (2011) A practical guide to evaluating colocalization in biological microscopy. Am J Physiol Cell Physiol 300:C723-742. https://doi.org/10.1152/ajpcell.00462.2010
14. Garza M, Piquet AL (2021) Update in autoimmune movement disorders: newly described antigen targets in autoimmune and paraneoplastic cerebellar ataxia. Front Neurol 12:683048. https://doi.org/10.3389/fneur.2021.683048
15. Gilliam FG, Hecimovic H, Gentry MS (2021) Serotonergic therapy in epilepsy. Curr Opin Neurol 34:206–212. https://doi.org/10.1097/WCO.0000000000000901
16. Gould L, Delavale V, Plovnick C, Wisniewski T, Devinsky O (2023) Are brief febrile seizures benign? A systematic review and narrative synthesis. Epilepsia 64:2539–2549. https://doi.org/10.1111/epi.17720
17. Gould L, Reid CA, Rodriguez AJ, Devinsky O (2024) Group fSVW video analyses of sudden unexplained deaths in toddlers. Neurology 102:e208038. https://doi.org/10.1212/WNL.0000000000208038
18. Guiard BP, Di Giovanni G (2015) Central serotonin-2A (5-HT2A) receptor dysfunction in depression and epilepsy: the missing link? Front Pharmacol 6:46. https://doi.org/10.3389/fphar.2015.00046
19. Gunnersen JM, Kim MH, Fuller SJ, De Silva M, Britto JM, Hammond VE et al (2007) Sez-6 proteins affect dendritic arborization patterns and excitability of cortical pyramidal neurons. Neuron 56:621–639. https://doi.org/10.1016/j.neuron.2007.09.018
20. Halvorsen M, Gould L, Wang X, Grant G, Moya R, Rabin R et al (2021) De novo mutations in childhood cases of sudden unexplained death that disrupt intracellular Ca^{2+} regulation. Proc Natl Acad Sci 118:e2115140118. https://doi.org/10.1073/pnas.2115140118
21. Hansen KF, Sakamoto K, Pelz C, Impey S, Obrietan K (2014) Profiling status epilepticus-induced changes in hippocampal RNA expression using high-throughput RNA sequencing. Sci Rep 4:6930. https://doi.org/10.1038/srep06930
22. Heberle H, Meirelles GV, da Silva FR, Telles GP, Minghim R (2015) InteractiVenn: a web-based tool for the analysis of sets through venn diagrams. BMC Bioinformatics 16:169. https://doi.org/10.1186/s12859-015-0611-3
23. Hefti MM, Cryan JB, Haas EA, Chadwick AE, Crandall LA, Trachtenberg FL et al (2016) Hippocampal malformation associated with sudden death in early childhood: a neuropathologic study: part 2 of the investigations of the San Diego SUDC research project. Forensic Sci Med Pathol 12:14–25. https://doi.org/10.1007/s12024-015-9731-3
24. Hefti MM, Kinney HC, Cryan JB, Haas EA, Chadwick AE, Crandall LA et al (2016) Sudden unexpected death in early childhood: general observations in a series of 151 cases: Part 1 of the investigations of the San Diego SUDC research project. Forensic Sci Med Pathol 12:4–13. https://doi.org/10.1007/s12024-015-9724-2
25. Hesdorffer DC, Crandall LA, Friedman D, Devinsky O (2015) Sudden unexplained death in childhood: a comparison of cases with and without a febrile seizure history. Epilepsia 56:1294–1300. https://doi.org/10.1111/epi.13066
26. Hetman M, Slomnicki LP (2019) Ribosomal biogenesis as an emerging target of neurodevelopmental pathologies. J Neurochem 148:325–347. https://doi.org/10.1111/jnc.14576
27. Hornung J-P (2012) Chapter 11 - raphe nuclei. In: Mai JK, Paxinos G (eds) The human nervous system (3rd Edition). Academic Press, San Diego pp 401–424. https://doi.org/10.1016/B978-0-12-374236-0.10011-2
28. Johnson ECB, Dammer EB, Duong DM, Ping L, Zhou M, Yin L et al (2020) Large-scale proteomic analysis of Alzheimer's disease brain and cerebrospinal fluid reveals early changes in energy metabolism associated with microglia and astrocyte activation. Nat Med 26:769–780. https://doi.org/10.1038/s41591-020-0815-6
29. Kather A, Holtbernd F, Brunkhorst R, Hasan D, Markewitz R, Wandinger KP et al (2022) Anti-SEZ6L2 antibodies in paraneoplastic cerebellar syndrome: case report and review of the literature. Neurol Res Pract 4:54. https://doi.org/10.1186/s42466-022-00218-4
30. Kaur S, De Luca R, Khanday MA, Bandaru SS, Thomas RC, Broadhurst RY et al (2020) Role of serotonergic dorsal raphe neurons in hypercapnia-induced arousals. Nat Commun 11:2769. https://doi.org/10.1038/s41467-020-16518-9
31. Kinney HC, Haynes RL (2019) The serotonin brainstem hypothesis for the sudden infant death syndrome. J Neuropathol Exp Neurol 78:765–779. https://doi.org/10.1093/jnen/nlz062
32. Kinney HC, Poduri AH, Cryan JB, Haynes RL, Teot L, Sleeper LA et al (2016) Hippocampal formation maldevelopment and sudden unexpected death across the pediatric age spectrum. J Neuropathol Exp Neurol 75:981–997. https://doi.org/10.1093/jnen/nlw075
33. Kinney HC, Richerson GB, Dymecki SM, Darnall RA, Nattie EE (2009) The brainstem and serotonin in the sudden infant death syndrome. Annu Rev Pathol 4:517–550. https://doi.org/10.1146/annurev.pathol.4.110807.092322
34. Kon FC, Vázquez RZ, Lang A, Cohen MC (2020) Hippocampal abnormalities and seizures: a 16-year single center review of sudden unexpected death in childhood, sudden unexpected death in epilepsy and SIDS. Forensic Sci Med Pathol 16:423–434. https://doi.org/10.1007/s12024-020-00268-7
35. Kumar GA, Chattopadhyay A (2021) Membrane cholesterol regulates endocytosis and trafficking of the serotonin. Biochim

Biophys Acta Mol Cell Biol Lipids 1866:158882. https://doi.org/10.1016/j.bbalip.2021.158882
36. Lake BB, Chen S, Sos BC, Fan J, Kaeser GE, Yung YC et al (2018) Integrative single-cell analysis of transcriptional and epigenetic states in the human adult brain. Nat Biotechnol 36:70–80. https://doi.org/10.1038/nbt.4038
37. Leitner D, Pires G, Kavanagh T, Kanshin E, Askenazi M, Ueberheide B et al (2024) Similar brain proteomic signatures in Alzheimer's disease and epilepsy. Acta Neuropathol 147:27. https://doi.org/10.1007/s00401-024-02683-4
38. Leitner DF, Devore S, Laze J, Friedman D, Mills JD, Liu Y et al (2022) Serotonin receptor expression in hippocampus and temporal cortex of temporal lobe epilepsy patients by postictal generalized electroencephalographic suppression duration. Epilepsia 63:2925–2936. https://doi.org/10.1111/epi.17400
39. Leitner DF, Faustin A, Verducci C, Friedman D, William C, Devore S et al (2021) Neuropathology in the North American sudden unexpected death in epilepsy registry. Brain Commun 3:fcab192. https://doi.org/10.1093/braincomms/fcab192
40 Leitner DF, Kanshin E, Askenazi M, Faustin A, Friedman D, Devore S et al (2022) Raphe and ventrolateral medulla proteomics in epilepsy and sudden unexpected death in epilepsy. Brain Commun 4:fcac186. https://doi.org/10.1093/braincomms/fcac186
41. Leitner DF, Kanshin E, Askenazi M, Siu Y, Friedman D, Devore S et al (2022) Pilot study evaluating everolimus molecular mechanisms in tuberous sclerosis complex and focal cortical dysplasia. PLoS ONE 17:e0268597. https://doi.org/10.1371/journal.pone.0268597
42. Leitner DF, McGuone D, William C, Faustin A, Askenazi M, Snuderl M et al (2021) Blinded review of hippocampal neuropathology in sudden unexplained death in childhood reveals inconsistent observations and similarities to explained pediatric deaths. Neuropathol Appl Neurobiol. https://doi.org/10.1111/nan.12746
43. Leitner DF, Mills JD, Pires G, Faustin A, Drummond E, Kanshin E et al (2021) Proteomics and transcriptomics of the hippocampus and cortex in SUDEP and high-risk SUDEP patients. Neurology. https://doi.org/10.1212/WNL.0000000000011999
44. Leitner DF, William C, Faustin A, Askenazi M, Kanshin E, Snuderl M et al (2022) Proteomic differences in hippocampus and cortex of sudden unexplained death in childhood. Acta Neuropathol 143:585–599. https://doi.org/10.1007/s00401-022-02414-7
45. Ma H, Yu Q, Shen Y, Lian X, Gu L, Wang Y et al (2022) Dorsal raphe nucleus to pre-Bötzinger complex serotonergic neural circuit is involved in seizure-induced respiratory arrest. iScience 25:105228. https://doi.org/10.1016/j.isci.2022.105228
46. JaEMBaHMaDM M (2012) Serotonergic signaling: multiple effectors and pleiotropic effects. Wiley Interdisciplinary Rev: Membrane Trans Signal 1:685–713. https://doi.org/10.1002/wmts.50
47. McGuone D, Crandall LG, Devinsky O (2020) Sudden unexplained death in childhood: a neuropathology review. Front Neurol 11:582051. https://doi.org/10.3389/fneur.2020.582051
48. McGuone D, Leitner D, William C, Faustin A, Leelatian N, Reichard R et al (2020) Neuropathologic changes in sudden unexplained death in childhood. J Neuropathol Exp Neurol 79:336–346. https://doi.org/10.1093/jnen/nlz136
49. Millan MJ, Marin P, Bockaert J, Mannoury la Cour C (2008) Signaling at G-protein-coupled serotonin receptors: recent advances and future research directions. Trends Pharmacol Sci 29:454–464. https://doi.org/10.1016/j.tips.2008.06.007
50. Miyazaki T, Hashimoto K, Uda A, Sakagami H, Nakamura Y, Saito SY et al (2006) Disturbance of cerebellar synaptic maturation in mutant mice lacking BSRPs, a novel brain-specific receptor-like protein family. FEBS Lett 580:4057–4064. https://doi.org/10.1016/j.febslet.2006.06.043
51. Mueller SG, Nei M, Bateman LM, Knowlton R, Laxer KD, Friedman D et al (2018) Brainstem network disruption: a pathway to sudden unexplained death in epilepsy? Hum Brain Mapp 39:4820–4830. https://doi.org/10.1002/hbm.24325
52. Mulley JC, Iona X, Hodgson B, Heron SE, Berkovic SF, Scheffer IE et al (2011) The role of seizure-related SEZ6 as a susceptibility gene in febrile seizures. Neurol Res Int 2011:917565. https://doi.org/10.1155/2011/917565
53 Nikolić J, Vukojević K, Šoljić V, Mišković J, Orlović Vlaho M, Saraga-Babić M et al (2023) Expression patterns of serotonin receptors 5-HT1A, 5-HT2A, and 5-HT3A during human fetal lung development. Int J Mol Sci. https://doi.org/10.3390/ijms24032965
54. Paterson DS, Darnall R (2009) 5-HT2A receptors are concentrated in regions of the human infant medulla involved in respiratory and autonomic control. Auton Neurosci 147:48–55. https://doi.org/10.1016/j.autneu.2009.01.004
55. Paterson DS, Thompson EG, Kinney HC (2006) Serotonergic and glutamatergic neurons at the ventral medullary surface of the human infant: observations relevant to central chemosensitivity in early human life. Auton Neurosci 124:112–124. https://doi.org/10.1016/j.autneu.2005.12.009
56. Paxinos G, Xu-Feng H, Sengul G, Watson C (2012) Chapter 8 - organization of brainstem nuclei. In: Mai JK, Paxinos G (eds) The human nervous system (3rd Edition). Academic Press, San Diego p. 260–327. https://doi.org/10.1016/B978-0-12-374236-0.10008-2
57. Petrucci AN, Joyal KG, Chou JW, Li R, Vencer KM, Buchanan GF (2021) Post-ictal generalized EEG suppression is reduced by enhancing dorsal raphe serotonergic neurotransmission. Neuroscience 453:206–221. https://doi.org/10.1016/j.neuroscience.2020.11.029
58. Pfister AS (2019) Emerging role of the nucleolar stress response in autophagy. Front Cell Neurosci 13:156. https://doi.org/10.3389/fncel.2019.00156
59. Pires G, Leitner D, Drummond E, Kanshin E, Nayak S, Askenazi M et al (2021) Proteomic differences in the hippocampus and cortex of epilepsy brain tissue. Brain Commun 3:fcab021. https://doi.org/10.1093/braincomms/fcab021
60. Punda H, Mardesic S, Filipovic N, Kosovic I, Benzon B, Ogorevc M et al (2021) Expression pattern of 5-HT (Serotonin) receptors during normal development of the human spinal cord and ganglia and in fetus with cervical spina bifida. Int J Mol Sci. https://doi.org/10.3390/ijms22147320
61. Richerson GB (2004) Serotonergic neurons as carbon dioxide sensors that maintain pH homeostasis. Nat Rev Neurosci 5:449–461. https://doi.org/10.1038/nrn1409
62. Rios-Fuller TJ, Mahe M, Walters B, Abbadi D, Pérez-Baos S, Gadi A et al (2020) Translation regulation by eIF2α phosphorylation and mTORC1 signaling pathways in non-communicable diseases (NCDs). Int J Mol Sci. https://doi.org/10.3390/ijms21155301
63. Roy A, Millen KJ, Kapur RP (2020) Hippocampal granule cell dispersion: a non-specific finding in pediatric patients with no history of seizures. Acta Neuropathol Commun 8:54. https://doi.org/10.1186/s40478-020-00928-3
64. Schwarzacher SW, Rüb U, Deller T (2011) Neuroanatomical characteristics of the human pre-Bötzinger complex and its involvement in neurodegenerative brainstem diseases. Brain 134:24–35. https://doi.org/10.1093/brain/awq327
65. Seyfried NT, Dammer EB, Swarup V, Nandakumar D, Duong DM, Yin L et al (2017) A multi-network approach identifies protein-specific co-expression in asymptomatic and symptomatic Alzheimer's disease. Cell Syst 4:60-72.e64. https://doi.org/10.1016/j.cels.2016.11.006
66. Smith DK, Sadler KP, Benedum M (2019) Febrile seizures: risks, evaluation, and prognosis. Am Fam Physician 99:445–450

67. Smith HR, Leibold NK, Rappoport DA, Ginapp CM, Purnell BS, Bode NM et al (2018) Dorsal raphe serotonin neurons mediate CO. J Neurosci 38:1915–1925. https://doi.org/10.1523/JNEUROSCI.2182-17.2018
68. Teranishi Y, Inoue M, Yamamoto NG, Kihara T, Wiehager B, Ishikawa T et al (2015) Proton myo-inositol cotransporter is a novel γ-secretase associated protein that regulates Aβ production without affecting Notch cleavage. FEBS J 282:3438–3451. https://doi.org/10.1111/febs.13353
69. Thom M, Michalak Z, Wright G, Dawson T, Hilton D, Joshi A et al (2016) Audit of practice in sudden unexpected death in epilepsy (SUDEP) post mortems and neuropathological findings. Neuropathol Appl Neurobiol 42:463–476. https://doi.org/10.1111/nan.12265
70. Torretta E, Arosio B, Barbacini P, Capitanio D, Rossi PD, Moriggi M et al (2021) Novel insight in idiopathic normal pressure hydrocephalus (iNPH) biomarker discovery in CSF. Int J Mol Sci. https://doi.org/10.3390/ijms22158034
71. Tyanova S, Temu T, Sinitcyn P, Carlson A, Hein MY, Geiger T et al (2016) The Perseus computational platform for comprehensive analysis of (prote)omics data. Nat Methods 13:731–740. https://doi.org/10.1038/nmeth.3901
72. Uldry M, Steiner P, Zurich MG, Béguin P, Hirling H, Dolci W et al (2004) Regulated exocytosis of an H+/myo-inositol symporter at synapses and growth cones. EMBO J 23:531–540. https://doi.org/10.1038/sj.emboj.7600072
73. Van Oekelen D, Megens A, Meert T, Luyten WH, Leysen JE (2003) Functional study of rat 5-HT2A receptors using antisense oligonucleotides. J Neurochem 85:1087–1100. https://doi.org/10.1046/j.1471-4159.2003.01738.x
74. Vashishta A, Slomnicki LP, Pietrzak M, Smith SC, Kolikonda M, Naik SP et al (2018) RNA polymerase 1 is transiently regulated by seizures and plays a role in a pharmacological kindling model of epilepsy. Mol Neurobiol 55:8374–8387. https://doi.org/10.1007/s12035-018-0989-9
75. Yaguchi H, Yabe I, Takahashi H, Watanabe M, Nomura T, Kano T et al (2017) Sez6l2 regulates phosphorylation of ADD and neuritogenesis. Biochem Biophys Res Commun 494:234–241. https://doi.org/10.1016/j.bbrc.2017.10.047
76. Zhang B, Peng X, Sun X, Guo Y, Li T (2022) Environmentally-relevant concentrations of the antipsychotic drugs sulpiride and clozapine induce abnormal dopamine and serotonin signaling in zebrafish brain. Sci Rep 12:17973. https://doi.org/10.1038/s41598-022-22169-1
77. Zhang H, Zhao H, Zeng C, Van Dort C, Faingold CL, Taylor NE et al (2018) Optogenetic activation of 5-HT neurons in the dorsal raphe suppresses seizure-induced respiratory arrest and produces anticonvulsant effect in the DBA/1 mouse SUDEP model. Neurobiol Dis 110:47–58. https://doi.org/10.1016/j.nbd.2017.11.003